Available online at www.sciencedirect.com

ScienceDirect

Current Opinion in
Colloid & Interface Science

Elasticity and stability of shape-shifting structures

Douglas P. Holmes

Abstract

As we enter the age of designer matter — where objects can morph and change shape on command — what tools do we need to create shape-shifting structures? At the heart of an elastic deformation is the combination of dilation and distortion or stretching and bending. The competition between the latter can cause elastic instabilities, and over the last fifteen years, these instabilities have provided a multitude of ways to prescribe and control shape change. Buckling, wrinkling, folding, creasing, and snapping have become mechanisms that when harmoniously combined enable mechanical metamaterials, self-folding origami, ultralight and ultrathin kirigami, and structures that appear to grow from one shape to another. In this review, I aim to connect the fundamentals of elastic instabilities to the advanced functionality currently found within mechanical metamaterials.

Addresses

Department of Mechanical Engineering, Boston University, Boston, MA, 02215, USA

Corresponding author: Holmes, Douglas P (dpholmes@bu.edu)
URL: http://www.bu.edu/moss

Current Opinion in Colloid & Interface Science 2019, **40**:118–137

This review comes from a themed issue on **Particle Systems**

Edited by **Stefano Sacanna**, **Patrick Spicer** and **Krassimir Velikov**

For a complete overview see the Issue and the Editorial

https://doi.org/10.1016/j.cocis.2019.02.008

Keywords

Elasticity, Instability, Buckling, Snapping, Mechanical metamaterials, Origami and kirigami.

Introduction

How do objects change shape? This question has formed the basis of entire branches of mechanics and physics dating back centuries, and so it is reasonable to wonder what new questions and challenges remain. To drastically change an object's shape, it should possess some degree of *softness* — either in a material sense, for example, having a low elastic modulus, or in a geometric sense, for example, having slenderness. This softness comes at a price — large deformations introduce nonlinear responses and instabilities. Material nonlinearities are common with traditional engineering materials, that is, metals, wood, ceramics, which, whether they are brittle or ductile, will tend to irreversibly deform in response to small strains, either by fracturing or flowing plastically. Softer materials such as rubbers, gels, and biological tissues can often withstand moderate amounts of strain without reaching a material limit, and so they can reversibly withstand elastic instabilities without permanent deformation, exhibiting geometric nonlinearities by bending, buckling, wrinkling, creasing, and crumpling. It is perhaps no surprise then that a resurgence in studying elastic instabilities coincided with the emergence of new, simple, and inexpensive ways to prepare soft elastomers in any desired shape and size, thus enabling researchers to study how instabilities could perform useful functions. Now, the study of how to utilize elastic instabilities for mechanical functionality brings together the disciplines of soft matter physics, mechanics, applied mathematics, biology, and materials science with the aim to extend our understanding of structural stability for generating both form and function.

Elasticity of slender structures

Stretching and bending

Slenderness, embodied by the canonical forms, rods, plates, and shells, provides the most direct way to deform a structure, as the reduced dimensionality enables large deformations while the material stress remains low, that is, $\sigma/E \ll 1$, where σ is the maximum principal stress and E is Young's elastic modulus. Thin structures are highly susceptible to instability, and this is due in large part to their tendency to deform by bending.[1] The fact that these structures are by definition thinner in one dimension than the other two motivated the development of models of elastic deformation of lower spatial dimension, that is, reduced-order models, to describe slender structures, such as rods, plates, and shells. With a rod being the simplest of these forms, we can develop some intuition for how thin structures deform by looking at the strain energy of a thin elastic rod. Reduced-order models of slender structures have a common form: a stretching energy $\mathcal{U}_s$, which accounts for extension or compression of the middle surface of the rod and is linear in the rod thickness, h, and a bending energy $\mathcal{U}_b$, which accounts

[1] Readers interested in a more thorough understanding of the ideas presented throughout this review should consult the Supplementary Information [1].

for the curvature change of the deformed rod, and is dependent on h^3. The strain energy of a thin rod will scale as [1]

$$\mathscr{U} \sim \underbrace{Y \int \varepsilon^2 \mathrm{d}\omega}_{\mathscr{U}_s} + \underbrace{B \int \kappa^2 \mathrm{d}\omega}_{\mathscr{U}_b} \quad (1)$$

where $Y = Eh/(1-\nu^2)$ is the stretching rigidity, $B = Eh^3/[12(1-\nu^2)]$ is the bending rigidity, ν is Poisson's ratio, and $\mathrm{d}\omega$ is the area element. To gain some physical intuition about a particular problem, it is often adequate to simply consider how the relevant energies scale. For instance, by simply comparing the stretching and bending energies, we see that $\mathscr{U}_b/\mathscr{U}_s \sim h^2(\kappa/\varepsilon)^2$, where κ is the average curvature induced by bending the rod (units of reciprocal length), and ε is the average strain induced when stretching the rod (unitless). Because the rod is thin, this quantity must be very, very small, indicating that it is far easier to bend a thin structure than it is to stretch it. This insight helps explain why thin structures are prone to instability: if you try to shorten the length of a thin rod by compressing it, the rod would much rather bend than be compressed, and to bend, it must buckle.

The remainder of this review deals with the challenge of controlling the shape change of a structure while overcoming the constraints on bending and stretching it. An overview of how researchers have overcome these constraints is presented in Figure 1, which highlights how tailoring materials, geometry, and topology can enable structures to stretch and bend in unconventional ways, and how elastic instabilities enable structural morphing and metamaterial behaviors such as negative Poisson ratio and negative swelling. By building upon the fundamentals of elasticity (Section Elasticity of slender structures) and harnessing elastic instabilities for enhanced functionality (Section Elastic instability phenomena), we are now ushering in an age of programmable matter (Section Programmable matter). The multitude of approaches for changing an object's shape share similar techniques — mechanical metamaterials are built around buckling and snapping mechanisms, origami and kirigami create local regions that bend easily, shape-shifting structures swell more or less locally — and the purpose of this review is to provide the reader the insight to see the underlying principles that govern shape change.

Scaling

Using the scaling relations of a thin structure's stretching and bending energy, we were able to quickly see why thin objects bend rather than stretch. This approach can be useful for understanding the relevant physics in a whole range of phenomena, and we will review some of the most relevant examples here.

Elastogravity length

Let's consider a simple question: If I slide a sheet of paper over the edge of my desk, at what length will this

Figure 1

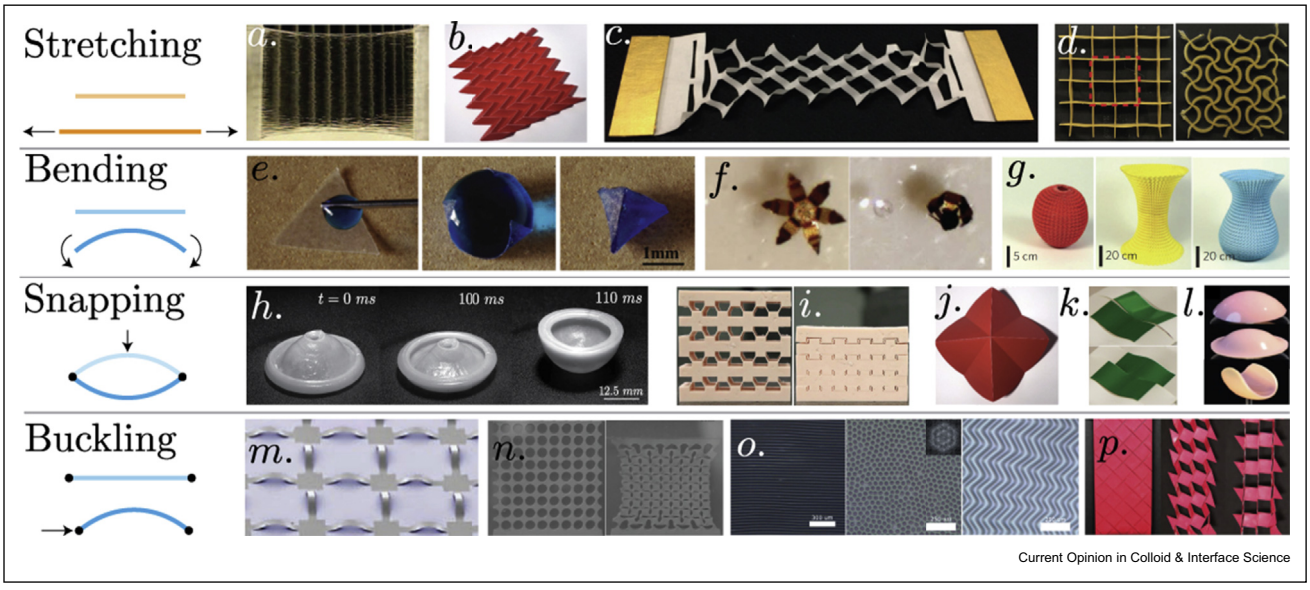

Stretching. **(a)** Highly stretchable gel using double-network gels [2]. **(b)** Miura-ori fold [3]. **(c)** Extremely stretchable thin sheets via kirigami [4]. **(d)** Negative swelling gels [5]. Bending. **(e)** Capillary origami [6]. **(f)** Tetherless microgrippers [7]. **(g)** Programming curvature with origami [8]. Snapping. **(h)** Snapping poppers [9]. **(i)** Snapping elements that absorb elastic strain energy [10]. **(j)** Bistable water bomb fold [3]. **(k)** Bistable kirigami unit cells [11]. **(l)** Swelling-induced snapping shells [12]. Buckling. Buckled silicon membranes [13]. **(n)** Negative Poisson ratio [14]. **(o)** Wrinkle patterns [15]. **(p)** Buckling-induced kirigami [16].

Figure 2

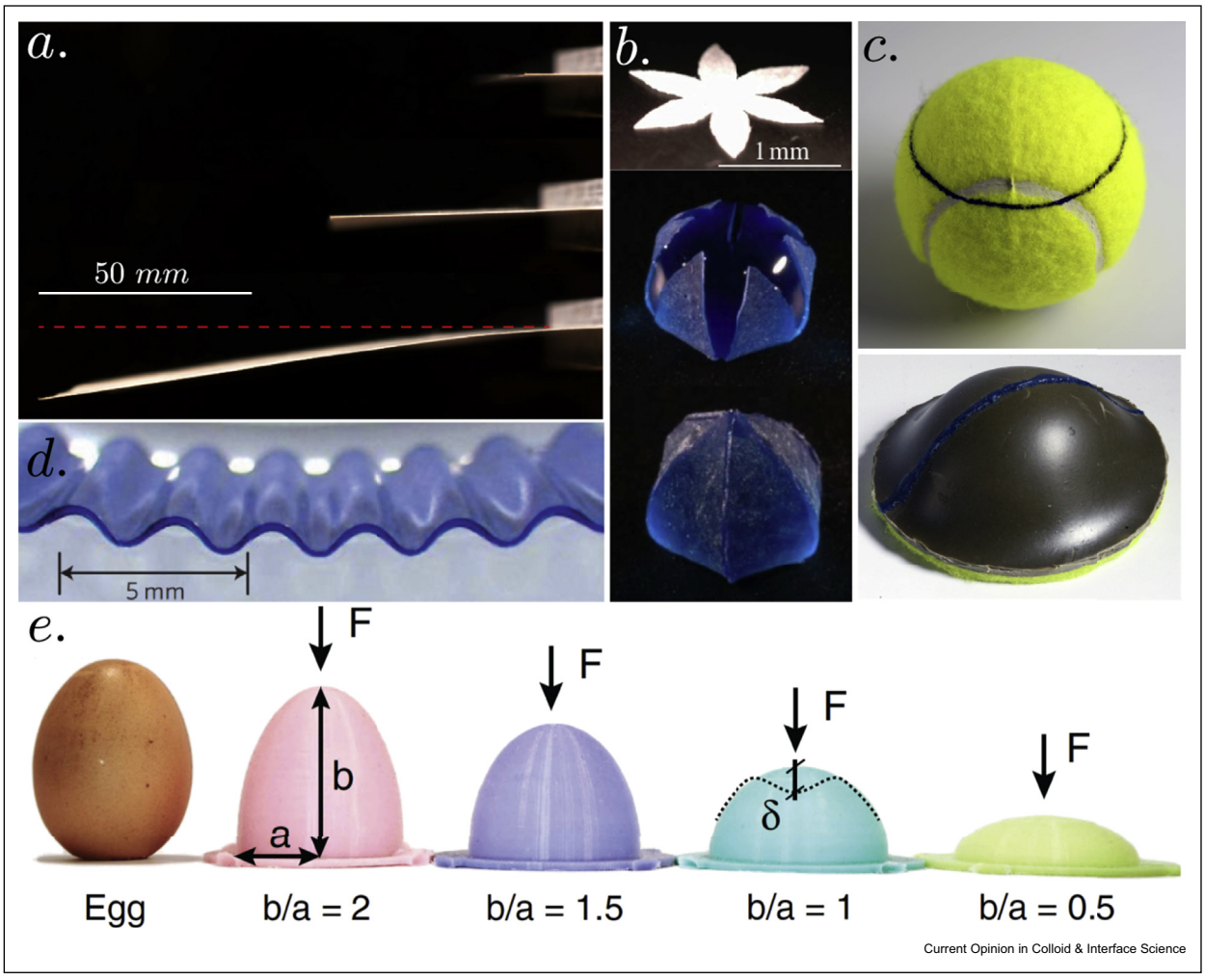

Characteristic length scales in elasticity. **(a)** Demonstration of the elastogravity length with a sheet of paper. **(b)** Elastocapillary encapsulation adapted from the study by Py [6]. **(c)** Snap-through eversion of a spherical cap, demonstrated with a tennis ball, adapted from the study by Taffetani et al. [44]. **(d)** Wrinkles on a soft substrate adapted from the study by Baru et al. [45]. (e) A demonstration of geometric rigidity from the study by Lazarus et al. [46].

sheet begin to bend under its own weight? Gravity is the relevant force here, and we know that the gravitational potential energy scales as

$$\mathscr{U}_g \sim \rho g h \int \delta \mathrm{ds} \tag{2}$$

where ρ is the volumetric density of the paper, h is the paper thickness, g is the acceleration due to gravity, and δ is the distance over which gravity is acting. To determine when gravity will bend a thin sheet, we need to consider the term κ in Eq. (1) more carefully. Here, bending represents a vertical deflection δ occurring relative to our unknown length ℓ. Because κ is a curvature, for small deflections, we may write $\kappa \approx \partial^2\delta/\partial x^2$, such that from dimensional analysis, we may write $\kappa \sim \delta/\ell^2$. We expect the sheet of paper will bend when the energetic potential from gravity is on the same order as the energetic resistance to bending, and so by equating Eq. (2) and $\mathscr{U}_b$, we arrive at a characteristic elastogravity length scale[2] [17,18]

$$\ell_{eg} \sim \left(\frac{B}{\rho g h}\right)^{1/3} \tag{3}$$

Typical office paper has a bending rigidity of B=40 mN•m, thickness of h=0.1 mm, and density of ρ=800 kg/m^3, meaning that an overhang of about 37.1 mm (1.46 in) will cause the paper to start to sag (Figure 2a). Beyond being a useful back-of-the-envelope calculation,

[2] Depending on the choice of B (which often takes the form of $B \sim Er^4$ for a rod) and the choice of ρ (which may be taken to be an areal density), this exponent may change accordingly.

the elastogravity length has been shown to play an important role in determining the wavelength of wrinkling surfactant monolayers [19], the ability of thin elastic sheets to 'grab' water [20], the curling [21] and twisting [22] of an elastic rod, the viscous peeling of plates [23], and the buckling [24] and wrinkling [25] of elastic sheets on water.

This balance of bending and gravity is also what determines the length of curly hair [26,27]. If the curl is treated as a circular spring that is opening under the force of gravity, the bending stiffness of the hair will be $k_{\text{curl}} \sim EI\kappa_n^3$, where κ_n is the curvature of the curl, or the intrinsic, natural curvature of the hair. Gravity acts upon each curl by ρgAL, where ρ is the density (mass/volume), A is the cross sectional area of the hair, and L is the total length of the hair. Each individual curl, or circular spring, will open by an amount $z_{\text{curl}} \sim \rho gAL/k_{\text{curl}}$, and if there are n curls, such that $n \sim L\kappa_n$, the vertical displacement of the free end of the hair should be Eq., 4 as given in the study by Audoly and Pomeau [26].

$$z \sim \frac{\rho gAL^2}{EI\kappa_n^2} \tag{4}$$

A similar argument can be used to design a Slinky. A Slinky is little more than a very floppy spring, and one of the most iconic features of this toy is that it can be bent into an arch. The bending energy for this discrete structure is slightly different than the continuous form given by $\mathscr{U}_b$ [28]; however, the concept is the same. Balancing the spring's effective bending rigidity against the gravitational potential yields indicates that this Slinky would need 71 rings to form a stable arch [28].[3] A Slinky typically has about 82 rings, so if you cut off about 11 or more, it will not be as fun to play with [28].

Elastocapillary length

We are familiar with fluids that deform thin structures through inertia, for example, consider the flapping of a flag in the wind [29]. In contrast, capillary forces are typically negligible at macroscopic scales. However, at micrometric and millimetric scales, surface tension can cause thin structures to bend. Therefore, a natural question to ask is at what length scale should I start to worry that capillary forces will deform my structure? Here, we are concerned with surface energy, which scales as

$$\mathscr{U}_\gamma \sim \gamma \int \mathrm{d}\omega \tag{5}$$

where γ is the surface tension of the liquid. The most elegant scenario to imagine was outlined by Roman and Bico in their review articles on this topic [30,31] in which they consider a thin strip spontaneously wrapping around a wet cylinder of radius R. For the strip to wrap around the cylinder, it must adopt a curvature of $\kappa \sim R^{-1}$. Here, again, we can balance bending energy $\mathscr{U}_b$ with surface energy (Eq. (5)) to arrive at a characteristic elastocapillary length [32,6].

$$\ell_{ec} \sim \left(\frac{B}{\gamma}\right)^{1/2} \tag{6}$$

With this simple example, the prefactor can be worked out to be exactly 1/2 [30], indicating that a sheet of office paper will spontaneously wrap around a cylinder wet with water (γ=72 mN•m) as long as its radius is greater than 372 mm (Figure 2b). Intuitively, this makes sense — paper is intrinsically flat, and so it should conform to a cylinder regardless of γ as $R \to \infty$, but below some critical R, bending will be too costly. The role of surface stresses is a highly active research area at the moment [33], and those interested in this brief primer would be better served reading the work of Roman and Bico [30,31], along with recent reviews on deforming soft solids [34], bundling fiber arrays [35], and approaches for using fluids to assemble structures [36].

Warping wafers

It is fair to say that one of the most classical examples of a shape-shifting structure is the bending of a bimetallic strip when it is heated [37]. While thin bimetallic strips and beams bend uniformly when subjected to a change in temperature, thin plates do not. This is perhaps familiar to those who have cooked in the oven with a metallic baking sheet, as it may buckle and warp when heated above a certain temperature. The bowing and warping of thin plates was a particularly important problem relating to the deposition of thin metallic films onto silicon wafers [38,39]. Homogenous heating of a bimetal plate will endow the plate with a homogenous natural curvature κ_n, causing it to bend into the segment of a spherical cap, which has a positive Gaussian curvature. Gauss's famous *Theorema Egregium* states that you cannot change the intrinsic curvature of a surface without stretching it, and so this deformation comes at the cost of stretching the plate's middle surface. Eventually, the energetic cost for the plate to bend into a cylinder becomes lower than the cost to continue stretching and bending into a spherical cap, and so the bowing wafer will buckle into a cylindrical shape [1,40].

The cost of stretching the plate's middle surface into a spherical cap is quantified by ε in Eq. (1), and this will scale as the square of the natural curvature κ_n times the plate radius r, such that $\varepsilon \sim (\ell\kappa_n)^2$ [41]. Alternatively, to avoid stretching, the disk will need to maintain its zero

[3] Using $n_r \sim \overline{EI}/(mgRh)$, with radius R=34.18mm, thickness h=0.67mm, mass per ring m=2.49g, and an experimentally measured effective bending rigidity of $\overline{EI} = 40 \times 10^{-6}$ N•m^2.

Gaussian curvature, which it can accomplish by bending into a cylinder. If it deforms into a cylindrical shape, the stretching energy is zero while the sheet has to suppress the curvature along one direction, such that the bending energy scales as it is written in Eq. (1), with $\kappa \sim \kappa_n$ [41]. By balancing the bending and stretching energies from Eq. (1), we find that the plate should buckle when [41].

$$\kappa_n \sim \frac{h}{\ell^2} \tag{7}$$

where for thermal problems, the natural curvature can be related to the temperature by calculating the curvature of a beam of given modulus and thickness ratios using Timoshenko's well-known result [37]. In addition, the prefactor of this equation has been worked out exactly for most plate geometries [41]. This scaling analysis also gives rise to a characteristic length scale that is relevant to the anticlastic curvature of bent plates [42,43] and boundary layers in thin shells. By simply inverting the relation, we find

$$\ell_{bl} \sim \sqrt{\frac{h}{k_n}} \sim \sqrt{hR} \tag{8}$$

where R is the radius of curvature of a given shell. This characteristic length is easy to identify in thin shells. Take a tennis ball, cut it in half, and turn it inside out (Figure 2c). The flat lip that forms along the boundary of the everted shell has a length on the order of ℓ_{bl}.

Snapping shells

In the previous section, I encouraged an experiment that involves cutting a tennis ball and turning it inside out to see if it remains stable. A natural question may be beginning at the ball's apex, how far down, that is, at what latitude from the north pole, should you cut through it to ensure that it can be turned inside out? Turning a shell inside out requires the middle surface of the shell to stretch as it is everted. Pushing on a shell of radius R, similar to a ping pong ball or water bottle, to a depth δ causes a dent with a characteristic length of $\ell_{bl} \sim \sqrt{\delta R}$ — the same scaling that appears in Eq. (8) — and this dent is equivalent to a locally everted segment of the shell. This gives us a measure of the stretching strain, with $\varepsilon \sim \delta^2/\ell_{bl}^2 \sim \delta/R$ [44]. Deflection of the apex of the shell can be estimated in terms of the geometry of the shell, with $\delta = R(1-\cos\alpha) \sim \alpha^2 R$, where α is the planar angle subtended between the pole and the free edge of the shell [44]. Now, the stretching energy of the shell can be found from Eq. (1) using $\varepsilon \sim \alpha^2$. To turn a shell inside out, it will adopt a new radius of curvature that is quite close to its original radius of curvature, and the main distinction is that material points that were originally on the outer (inner) surface of the shell are now being compressed (stretched). This comes at the cost of bending the shell, which according to Eq. (1) can be found using $\kappa \sim 1/R$. Balancing these two energies, and, for historical reasons, taking the fourth root of the result, gives rise to a dimensionless parameter that characterizes the shell [47,44].

$$\Lambda \sim [12(1-\nu)]^{1/4} \left(\frac{R}{h}\right)^{1/2} \alpha. \tag{9}$$

Shells with $\Lambda \gtrsim 5.75$ can be turned inside out, or everted, and remain that way — that is, they are bistable [44]. For a typical tennis ball, with R=33.15mm, h=3.3mm, and Poisson ratio of ν=1/2, that means cutting the ball at a height of 15 mm from its north pole will yield a bistable shell.

Wrinkles

Probably no instability is more responsible for the surge in research interest on the topic of this review over the last fifteen years than wrinkling [48–51]. Similar to the others we have encountered so far, this problem also has both a long history [52] and a myriad of potential utility [53]. It is quite easy to see the pattern characteristic of wrinkling by simply compressing the skin on the underside of your forearm between your thumb and index finger. What is immediately apparent is the formation of ridges that are all equally spaced by some distance λ and all seem to have approximately the same amplitude A (Figure 2d). Therefore, a natural question is what sets the spacing of these wrinkles? The physics at play here do not include gravity or a fluid, and balancing bending and stretching alone is not enough. This is a buckling problem, but one where a stiff film (skin) is resting on a softer substrate which is resisting deformation — that is, we can consider the mechanics of a beam on an elastic foundation [54]. Consider the outer portion of your skin to be a stiff plate resting on a substrate that behaves like a Winkler foundation [54]. We can write the strain energy of the foundation as

$$\mathscr{U}_f \sim K \int \delta^2 \mathrm{d}\omega \tag{10}$$

where K is the stiffness of the foundation and δ is its deflection. A wrinkle will adopt a vertical deflection δ relative to some unknown characteristic spacing λ. Therefore, the curvature of these wrinkles, which costs bending energy, will scale as $\kappa \sim \delta/\lambda^2$. The ratio of δ to λ is set by the lateral compression Δ of the plate and substrate relative to some initial length L. From geometry, we find that $\delta/\lambda \approx (\Delta/\pi^2 L)^{1/2}$, a relation that is referred to as the *slaving* condition [55,56]. If λ is large, the bending energy of the plate will be minimal; however, this would require a significant stretching of the substrate. If λ is small, the stretching of the substrate is minimal, yet this would require the plate to bend with very large curvatures. However, the ratio of δ/λ can remain fixed for a given compression if we allow for a deformation with multiple undulations. With this in mind, balancing $\mathscr{U}_b$ with Eq. (10), we expect that the wrinkles will have a wavelength of [49].

$$\lambda \sim \left(\frac{B}{K}\right)^{1/4} \tag{11}$$

For a wide variety of systems, this scaling works remarkably well. Translating this scaling to a quantitative prediction of the wrinkle wavelength of a stiff skin on a soft substrate requires some additional analysis and is described in more detail in the Supplementary Information. The substrate does not need to be solid; indeed a fluid will impart an effective elastic stiffness of $K \sim \rho g$, where ρ is the density of water [51]. For instance, if you consider placing a droplet of water on a thin film floating on a bath of water, wrinkles will form on the surface due to surface tension [51,57–60]. The characteristic scaling of the wrinkles remains consistent as the loading or displacement is increased; however, this small perturbation to the shape becomes a much larger perturbation to the stress field. This change in the stress field is quantified as a transition from the post-buckling near-threshold regime to the far-from-threshold regime [57,59,61]. In the far-from-threshold regime, the stress field is still nearly axisymmetric [62] and can be used to determine the shape and stiffness of loaded films [56]. Eventually, at a large enough load or displacement, the stress field breaks axisymmetry, and we experimentally observe a large number of wrinkles collapse into a small number of folds: a wrinkle-to-fold transition [63].[4]

Geometric rigidity

Before we learn about how to control and direct the deformations of slender structures, it is useful to understand where these structures derive their rigidity from. Perhaps the most pleasant demonstration of how changing shape can increase an object's rigidity is to simply pick up a slice of thin-crust pizza. The tip of the pizza will sag under the weight of gravity, and so we fold the pizza in half, forming a cylindrical shape with the generatrix running from the tip to the crust. This curvature makes it much more difficult for gravity to deform the pizza because it would have to induce bending in two directions which would require a change in Gaussian curvature — something too difficult for gravity to accomplish alone.

It has long been known that geometry alone can provide functionality, such as enhanced structural integrity — arches have been used in architecture to bear loads for over four thousand years, and these structures exhibit their rigidity due to their intrinsic curvature. Shell structures, such as domes, are no different. Research by Vella et al. [64,65] and Lazarus et al. [46] has shed light on the intimate connections between a shell's geometry and its mechanical behavior, demonstrating that tuning a shell's shape, rather than the materials, provides a straightforward way to enhance its ability to sustain a load. Consider a positively curved (e.g. spherical, ellipsoidal), pressurized shell loaded at its apex by a point force. The rigidity of the shell depends on both the depth of indentation relative to shell thickness and the degree of shell pressurization. In the limit of weakly pressurized shells, the classical stiffness of an unpressurized shell, first obtained by Reissner, are recovered [66,64,46], which find that the stiffness is dependent on the shell's Gaussian curvature $\mathscr{K}$. The shell's rigidity is correlated to the in-plane stretching of the shell [64], an energetically costly deformation. Consider an egg shell, which is effectively ellipsoidal. If we take the Gaussian curvature at any point on the shell to be the product of the two principle curvatures, then $\mathscr{K}$ will be largest at the north pole of the shell and lowest at the equator — therefore, the enhanced stiffness observed with compressing a chicken egg at its poles compared to its equator is a consequence of geometry-induced rigidity [46] (Figure 2e). In the limit of high pressure, the mean curvature $\mathscr{H}$, not the Gaussian curvature, governs the shell stiffness [65]. The absence of a dependence on $\mathscr{K}$ in the large deflections of highly pressurized shells implies that the internal pressure negates the effect of geometric rigidity.

Understanding how a shell's stiffness depends on both the degree of internal pressure and the extent of deformation may be an important tool for biomechanical characterization. An important question for quantifying the morphogenesis of cellular and multicellular structures is how to deconvolute measurements of the cell wall mechanics from measurements of the pressure caused by osmotic fluid flow through the cell wall [67], that is, turgor pressure. Vella et al. [64] demonstrated that their results on the indentation of pressurized elastic shells could characterize the turgor pressure within yeast cells, *viz. Saccharomyces cerevisiae*. Using the stiffness from the Reissner limit, a turgor pressure within the yeast cells was estimated that was consistent with those measured using other experimental techniques [68]. Preliminary work has begun on extending this analysis to the measurement of the elastic properties of tomato fruit cells [69] and plant tissues [70,71], and further development of this model to include different loading types may provide insight into the large deformations observed within artificial biological microcapsules, for example, refer to the study by Neubauer et al. [72] and the references therein.

Elastic instability phenomena

The scaling from Eq. (1) tells us that thin structures prefer to bend rather than stretch, and in doing so will often exhibit an elastic instability. The efficient design of thin and lightweight structures out of high-strength materials leads to a conundrum at the heart of

[4] This topic is discussed a bit more in the Supplemental Information.

structural engineering: an optimum design is by its very nature prone to instability. With ample evidence that structural instability plays an integral role in the morphogenesis of biological materials [73] — from fingerprint formation [74,75], to the folds in the cerebral cortex [76–78], to the tendril perversion in climbing plants [79] — it is perhaps more important than ever that scientists and engineers studying solid materials have a strong understanding of the mechanics of elastic stability.

Stability requires us to consider the internal exchange of energy within a structure, with the total potential energy consisting of the internal strain energy and the potential from the external loads, that is, $\mathscr{V} = \mathscr{U}_s + \mathscr{U}_b + \mathscr{P}$. We recall that the first variation of the total potential energy must be equal to zero for a structure to be in equilibrium, $\delta\mathscr{V} = 0$. This statement is equivalent to Newton's second law. Equilibrium does not ensure stability, however. It is possible to balance a ball on the apex of a steep hill, such that it is in equilibrium, but this equilibrium is unstable because any slight perturbation will cause the ball to role far away and not return. A ball resting at the bottom of a hill is of course stable because any perturbation to it, for example, rolling it slightly up the hill will cause it to return to its original position once the perturbation is removed. We can also speak of neutral equilibrium, which would refer to the ball resting on a flat surface — any perturbation will not change the ball's potential energy. With this simple analogy, we may recognize that these hills represent a potential energy landscape, and that we need to investigate the convexity or concavity of this landscape at an equilibrium point to determine if this equilibrium is stable or unstable, respectively. This requires us to investigate the character of the second variation of the total potential energy — a structure is stable if $\delta^2\mathscr{V} > 0$, unstable if $\delta^2\mathscr{V} < 0$, and neutral if $\delta^2\mathscr{V} = 0$ [1]. It is tempting to relate these ideas to finding the extrema and curvature of a function in ordinary calculus; however, energy is not a function, but rather a functional — a function of a function of a variable. Evaluating the character of a functional requires the tools from variational calculus, and perhaps the most enjoyable primer on the calculus of variations can be found in Feynman's lectures [80].

For an elastic structure under a conservative load, the critical point at which an instability occurs will always correspond to either a bifurcation ('buckling') or a limit point ('snapping'). Imperfections in the structure's shape or within the material, or the eccentricity of the load can cause bifurcation critical points to change in character to a limit point, suggesting that buckling is perhaps more the exception than the rule [81]. On the surface, it seems surprising that buckling problems are abound in the literature, whereas limit point problems appear far less frequently. There are, in general, two reasons for this imbalance. First, the distinction between bifurcations and limit points is not merely semantic: one mathematical tool that allows us to study bifurcations — namely, linear stability analysis — is impossible to use to study a limit point instability [82,83], making buckling problems far easier to analyze. Second, slender structures are most efficient if they carry their load in a primarily membrane state of stress — meaning the loads act to stretch or compress the middle surface of the thin object, and such configurations will typically fail by buckling rather than snapping [81]. The primary mathematical difference between a bifurcation and a limit point instability is this: A limit point occurs when the equilibrium position becomes unstable, and the structure moves to the closest, stable point on the same equilibrium path, while a bifurcation occurs when two equilibrium pathways intersect, and an exchange of stability occurs as the structure follows the stable equilibrium path. By way of a metaphor, I view snapping as akin to walking along a path in the woods and encountering a puddle that one must jump over to continue, while buckling represents a fork in the road, occurring when a new path appears. Concrete examples of these two generic instability phenomena are given in the Supplementary Information. For the chemist or physicist, these definitions may bring to mind a connection between these instabilities and phase transitions [84–86], wherein one could draw an analogy between a limit point instability and a first-order phase transition, and a bifurcation with a second-order phase transition. This is perhaps more useful conceptually than practically, but several similarities are shared. We will begin with snapping, which requires us to consider only one equilibrium path, whereas buckling requires the exchange of stability between two equilibrium paths.

Snapping

The snap-through instability presents an important mechanism for directed shape change in the design of shape-shifting structures. A recent review on this topic by Hu et al. will hopefully provide a nice compliment to the following discussion [87]. There have been demonstrations of actuating snap-through instabilities for just about every conceivable mechanical and nonmechanical stimulus, including temperature [88], light [89], acoustic excitation [90,91], elastomer or gel swelling [92–94,12], magnetic fields [95,96], fluid flow [97], surface tension or elastocapillarity [98], and electrical current with materials that include from ceramic (piezoelectric) [99,100], metallic (electrostatic) [101,102], and rubber (dielectric elastomers) [103,104,24,105]. Laminated composites of epoxy and carbon fiber or fiber glass may exhibit bistability or multistability while thermally curing [106–109]. Depending on the fiber orientation, the presence of the fiber embedded in the epoxy matrix may give these materials an orthotropic response, thus providing design criteria for the orientation of the stimulus chosen to

induce snapping [40]. Such structures may enable morphing components for wind turbines [110], mechanisms for swimming or flying [111], ventricular assist devices [112], and for lightweight, deployable structures [113,114]. In a similar manner, the orientation of the residual stress or prestress resulting from fabrication can alter the geometric criteria for bistability [115–117]. In addition, rapid prototyping techniques, such as 3D printing and laser cutting, have made it much easier to generate bistable structures on a wide range of scales. Of note is the elastomer-coating technique pioneered by Lee et al., [118] which has made the preparation of thin, spherical caps with nearly uniform thickness simple, fast, and affordable. With all of these ways to induce snapping, it is no surprise that it has found utility in a wide range of engineering fields.

Experimental results on the adhesion of 2D materials such as graphene and MoS_2 have indicated that there is a snap into adhesive contact between the film and a substrate containing roughness [119,120], which has enabled researchers to demonstrate that this instability may be a useful metrology tool to measure the material properties of 2D materials [121]. The snap-through instability has also been used to tune a material's properties in response to an applied load by altering the material's lattice structure to generate dramatic, dynamic increases in a material's stiffness [122]. On a slightly larger scale, there is interest in the microelectromechanical and nanoelectromechanical (MEMS and NEMS, respectively) communities to use the rapid snap-through of arches and shells in electromechanical systems [123] for accelerometers [124] or as a means to rapidly change a surface's texture or optical properties [92]. The precise placement of folds in thin sheets can generate a wide range of multistable structures, with the most fundamental being the water bomb [125–127,3], which has generic bistability for any number of creases [3]. In addition to traditional folding and cutting techniques, programming creases into a material through spatial variations in its thickness can enable bistability in folded shells — cylinders, spheres, or saddles [128]. One function that has drawn particular attention is the design of bistable structures as a means to capture, trap, or harness elastic strain energy [129,10,130]. This process may be amenable for use with soft elastomers [10], which can undergo very large snap-through instabilities without exhibiting material failure [103,131,104,105]. If these soft materials are used as actuators, rather than energy harvesters, the instability can be used to trigger large, nonlinear changes in shape, pressure, and extension within soft, fluidic actuators [132].

Buckling

The elastic buckling of a beam or plate provides a straightforward way to get large, reversible, out-of-plane deformations, which can be used for generating advanced functionality [133]. For instance, embedding a flexible plate within a microfluidic channel provides a means for mechanically actuated valving [134,135]. Buckled plates have been used to fabricate semiconductor nanoribbons for stretchable electronics [136–138]. In recent years [139–141], researchers have used this principle to fabricate single-wall carbon nanotube arches [142], single-crystalline silicon arches that were used as metal-oxide semiconductor field-effect transistors (MOSFETs) [143], and buckled lead zirconate titanate (PZT) ribbons for ceramic piezoelectric energy-harvesting devices [144]. Buckling bilayer plates can be used to generate shape-shifting structures [41] that may be used as soft grippers [145]. Buckling of shells has provided an intriguing way to control global shape [146,147,12] and local patterning [148–151], reduce aerodynamic drag [152,153], generate lock-and-key colloids that can selectively aggregate [154], form liquid crystal shell actuators [155], and pave the way for buckling microswimmers [156].

Wrinkles are what appear when a thin structure buckles and the soft substrate it is bound to constrains the amplitude of the out-of-plane deformation [52,48–51,53]. There are a variety of ways to fabricate wrinkled surfaces, but the underlying principle is simple: bond a stiff film containing residual compressive stress onto a compliant substrate. Some of the first experiments in this manner involved the deposition of a thin metallic film onto a polydimethylsiloxane (PDMS) substrate by electron beam evaporation [157,158]. This deposition locally heats the PDMS surface, expanding it equibiaxially. Upon cooling, this compressive stress causes the metallic film to buckle with wrinkles in a herringbone pattern that cover a large surface area. Wrinkles have long added functionality to structural materials, such as with their ability to damp the structural vibrations occurring on composite plates [159]. Similar to the buckled ribbons used for flexible electronics, these wrinkled plates enabled the fabrication of stretchable gold conductors [160], flexible-electronic devices using wrinkled ribbons [161,141,162], and wrinkled single-walled carbon nanotubes [163]. Sinusoidal wrinkles have been used to alter and tune friction [164,165], to fabricate tunable phase gratings [166], and to improve the metrology of thin films via the strain-induced elastic buckling instability for mechanical measurement (SIEBIMM) technique [167]. In addition, there is significant evidence within biological systems to suggest that patterned surfaces alter adhesion [168–171]. Wrinkles are not limited to stiff films on soft substrates and can appear by merely stretching [49] or twisting a thin sheet [172,173]. Control of the pattern topography is a crucial component for using these structured surfaces (Figure 1o). Linear stability of the cylindrical pattern reveals the emergence of hexagonal, triangular, and square modes, and the commonly observed herringbone pattern [174,175,15]. Finally, as

the amount of overstress, or confinement, of the compressed plate increases, the bending energy along the plate goes from being broadly distributed among wrinkles to being localized within sharper features [176,63,1].

Programmable matter

Mechanical metamaterials

Metamaterials are rationally designed structures composed of building blocks to enable functionality that cannot be found in natural materials [181]. While this term has been traditionally associated with electromagnetism and optics, the field has recently broadened to include elastostatic and elastodynamic metamaterials, collectively called mechanical metamaterials. There is an excellent review that will cover the details of this topic far better than I will do here, so I encourage the curious reader to seek out Bertoldi et al. [182]. In general, the underlying concept of a mechanical metamaterial is to use hierarchical structures, such as microscale or mesoscale geometric features, to alter the macroscopic deformation of an object. Foam has natural microscale features and its atypical mechanical response exhibits a negative Poisson ratio [183]. This auxetic behavior [184] has been explored in a variety of contexts, many of which use the buckling of microscale/mesoscale beams within the macroscale structure [185,14]. With the inclusion of additional constraints, this auxetic behavior can be finely tuned to provide a programmatic structural deformation with a tailored

Figure 3

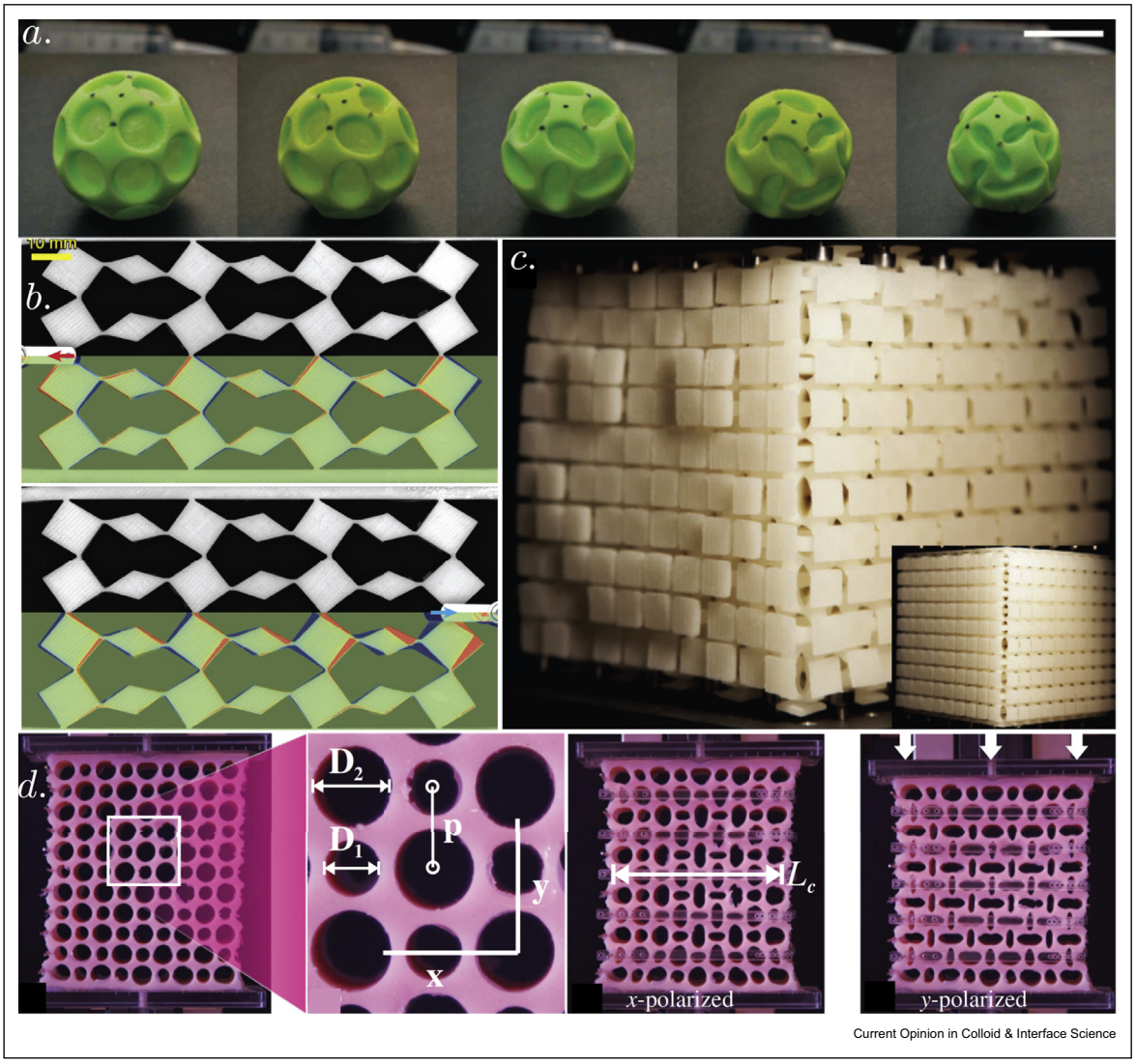

Mechanical metamaterials. **(a)** Spherical encapsulation with a 'buckliball', adapted from the study by Shim et al. [177]. **(b)** Static nonreciprocity in mechanical metamaterials [178]. (c) Programmatic shape change with a pixelated cube, adapted from the study by Coulais et al. [179]. (d) Programmatic structural polarity through external constraints, adapted from the study by Florijn et al. [180].

force–displacement response [180,186] (Figure 3d). Buckling of microstructural features to generate auxetic behavior can be extended from structured plates to structured shells to potentially encapsulate material [177] (Figure 3a). Instability is at the heart of mechanical metamaterials that exhibit negative compressibility, in which they contract while being loaded in tension, potentially enabling force amplification [187]. Buckling of subscale features becomes truly 'meta' when one considers the Euler buckling of metabeams [188], wherein the microstructure has a significant affect on the postbuckling response. More generally, precise control of pixelated structures provides a way to programmatically dictate a structure's deformation across multiple length scales [189] (Figure 3c). For example, the combinatorial design of specific building blocks can enable a cube to produce a smiling face in response to uniaxial compression [179]. Mechanical metamaterials are now veering closer to classical metamaterials by examining the role of topology in addition to geometry to transform shape and mechanical properties [190], with notable examples including structures to break the static reciprocity formalized by the Maxwell–Betti reciprocity theorem [178] (Figure 3b). Static reciprocity is the principle that describes why pushing a block on a table from the left will move it the same amount as pushing it from the right.

Origami and kirigami

Recall that Gauss's famous *Theorema Egregium* states that you cannot change the intrinsic curvature of a surface without stretching it, and we know from Eq. (1) that it is far easier to bend a thin object than stretch one. Therefore, if you want to stretch a thin object or wrap a sheet of paper around a soccer ball, what is one to do? One answer is to design regions that enable stretching, such as with the inclusion of folds and cuts. A review by Witten [191], which in my opinion did much to catalyze this entire discipline, describes at great lengths the way stress within thin sheets will localize into sharp folds, essentially acting as sacrificial regions in which a material begrudgingly stretches.[5] Understanding the mechanical nature of these folds guides their strategic incorporation into engineering systems. If these folds are precisely placed and sequentially actuated, they represent a means to develop advanced engineering structures. Taking inspiration from the Japanese art of origami, sequential folding has long been used in structured systems [192]. Deployable structures, used in space technologies, typically require damage-free actuation, reliable deformation, and autonomous or automated conformational change and have been used within small satellite deployable structures, deploy booms, and array panels [193,114]. Recent research has examined the mechanics of these foldable structures, with a focus on origami-inspired design [194,195], and thus, it may be useful to the reader to seek out the review article by Peraza-Hernandez et al. on this specific topic [196]. The fundamental mechanics of a fold [197] or more broadly a conical defect or singularity within a thin plate [198–201] are at the heart of understanding and designing origami mechanisms. While the geometric properties of a fold have been studied in great detail, the role of a material's properties in these systems has been largely overlooked to date. A notable exception is the work by Croll et al. [202] on the role of adhesion in crumpled structures. Unit cells of a repeating fold pattern provide origami building blocks [203] and enable the programmatic design of structural deformations [204–206], 3D shape-shifting [207], and folding-induced curvatures [8]. Such systems may exhibit multistability, as noted briefly in section on snapping [208,209].

The Miura-ori folding pattern is a well-known example of functional origami — a parallelogram of folds defined by two fold angles and two lengths, which enables the compact folding of a flat plate [210–212]. This functional array of pleated folds has been used for collapsable maps and deployable satellite arrays [213] and to increase the areal energy density of folded lithium-ion batteries [214]. Mathematicians and mechanicians alike have borrowed concepts from origami to create biomedical stents [215], nanostructured foldable electrodes [216], ultrathin high-resolution, folded optical lenses [217], photovoltaics [218], and materials with tunable coefficients of thermal expansion [219] and for folding rigid, thin-walled structures around hinges [220]. The techniques for generating folds include actuation by shape–memory alloys [221], light [222,223], microfluidic flow [224], and direct-printed wet-origami [225].

A natural extension of using folds inspired by origami to enable elaborate shape changes is to use cuts inspired by kirigami. Here, the fundamental behavior is governed by the nonlinear mechanics of thin frames [226]. With kirigami, the roles of topology [227] and geometry are once again at the heart of design rules that enable targeted shape changes [228–230]. Mechanics enters the picture by enabling these flat sheets to buckle into 3D structures when stretched or compressed beyond a critical point [16,231]. While lattice cuts have primarily been studied to date, with the work of Dias et al. being a notable exception [231], additional functionality was demonstrated with multiscale cuts, that is, kiri-kirigami [232], randomly oriented [233] and fractal cuts [234,235], and patterns that naturally interlock [236]. One of the primary demonstrations of functional shape change via kirigami is the extreme stretchability of thin sheets [237–239], which even translates to 2D

[5] There are important distinctions to be made about the structure of crumpled paper, including the formation of *developable* cones, or *d*–cones and the stretching ridges that connect them. Conversely, creases are localized deformations that seem similar to folds, yet are much sharper. Some of these details are covered in the SI.

materials, such as graphene [4]. Dias et al. [231] showed that to leading order, the out-of-plane deformation of a single cut is independent of the thickness of the sheet, providing mechanical insight into why this shape-shifting mechanism can scale down to the thinnest materials. Kirigami-inspired cut patterns have enabled the fabrication of photonic metamaterials [240], metamaterials with tunable material properties [11,241], smart adhesives [243], solar tracking devices [244], stretchable lithium-ion batteries [245], optical beam steering [246], shape-shifting structures [247], and ultra-lightweight linear actuators [231].

Shape-shifting structures

The control of geometry and elasticity to create adaptive, morphing structures paves the way for an era of designer materials [133]. We have reviewed the energetic limitations on bending and stretching structures, and we have seen how carefully chosen stretching regions — through, for example, origami and kirigami — enable a much wider range of shape changes. An alternative approach for shape-shifting structures is through the programmatic design of the volumetric strain within a material. An elegant example of controlling the spatial distribution of volumetric strain was recently demonstrated in the nonhomogenous pneumatic inflation and collapse of soft, elastic plates [254]. In general, this approach draws the closest analogy to synthetic structural growth. Swelling presents a simple and effective technique to spatially tune volumetric strain, while falling short of growth by not permanently adding mass to the reference elastomer, or reference configuration. Swelling is the infiltration of an elastic network with a favorable solvent, such that the characteristic size of the polymer chains, that is, their radius of gyration, dramatically increases. The balance of fluid movement and elastic response dictates the timescale over which swelling-induced phenomena will occur, and the ability for the fluid to swell the polymer network dictates the magnitude of stress imparted. Fluid flow within natural structures plays a crucial role in the morphology of growing tissues [255–257]; the opening of seed pods [258]; the shrinkage of mud [259] and moss [260]; and the curling of cartilage [261], leaves [262,263], and pine cones [264]. Porous thin films, such as fuel cell membranes [265], are highly susceptible to swelling-induced delamination and buckling, which cripple their functionality.

Swelling-induced deformations provide a means for shaping two-dimensional sheets into three-dimensional structures [248–250,266], with features spanning multiple length scales [267,268]. Differential swelling — where portions of the material locally swell more than others — have been used to create helical ribbons [269], cylinders [41], saddles [270,251], pinched spheres [12], and wavy strips and discs [271–273] (Figure 4). The shape selection process is nontrivial, and many efforts have focused on predicting what shape will emerge from programming the volumetric strain, often tailored using the metric tensor of the middle surface of a thin plate or shell [274–278,12]. The alternative, inverse problem — predicting what metric to program to achieve a specific 3D shape — may be even more desirable [279]. In addition to the contributions from the sheet's elastic energy, understanding the dynamic morphing of a swelling structure, such as the curling of paper [280,281], gels [282], and rubber [266,283], poses additional challenges [284,285]. An intricate photolithography technique, for example, halftone lithography, has been developed to scale this dynamic process down to create responsive, morphing structures on the micron scale [248]. The mechanics behind this structural morphing combines dynamic aspects of swelling, geometry, stability, and material properties, thereby creating a rich environment for experimental and theoretical insights. It is likely that building on the concept of programmable matter will inspire novel rapid-prototyping technologies, such as 3D 'inkjet' printing that uses small amounts of polymerizable solvents to create complex structures. Such ideas are already emerging in a technique known as 4D printing, where the fourth dimension represents the timescale corresponding to swelling [286,252,253,287–291].

Summary and outlook

Shape-shifting materials require working with and around the constraints of elasticity and utilizing nonlinearity to generate functionality. Most of what I have covered in this review does exactly that — overcoming the difficulty of stretching thin sheets by folding or cutting them, using the buckling and snapping of beams and plates and shells to generate metamaterial behavior, and playing with swelling to tune spatial distributions of strain. So, where do we go from here? Certainly, important research will continue in the areas we have covered at length, although new opportunities are beginning to emerge in a few specific areas. Much of the research captured by the moniker of *programmable matter* would be more aptly described as *programmed matter*. While at first glance this seems like a semantic distinction, I believe it is quite important. Very little work has produced materials that can be programmed and reprogrammed after fabrication or programmed in response to a mechanical computation or an array of external stimuli. How we take shape-shifting building blocks and produce generic structures that are truly programmable is an open question that will hopefully drive innovation in this area in the coming years.

I think one of the most significant areas of research going forward will focus on woven fabrics and knits for tailoring shape and properties [292,293], led in part by Prof. Matsumoto et al., and for example, such ideas are already enabling the form finding of grid shells [294].

Figure 4

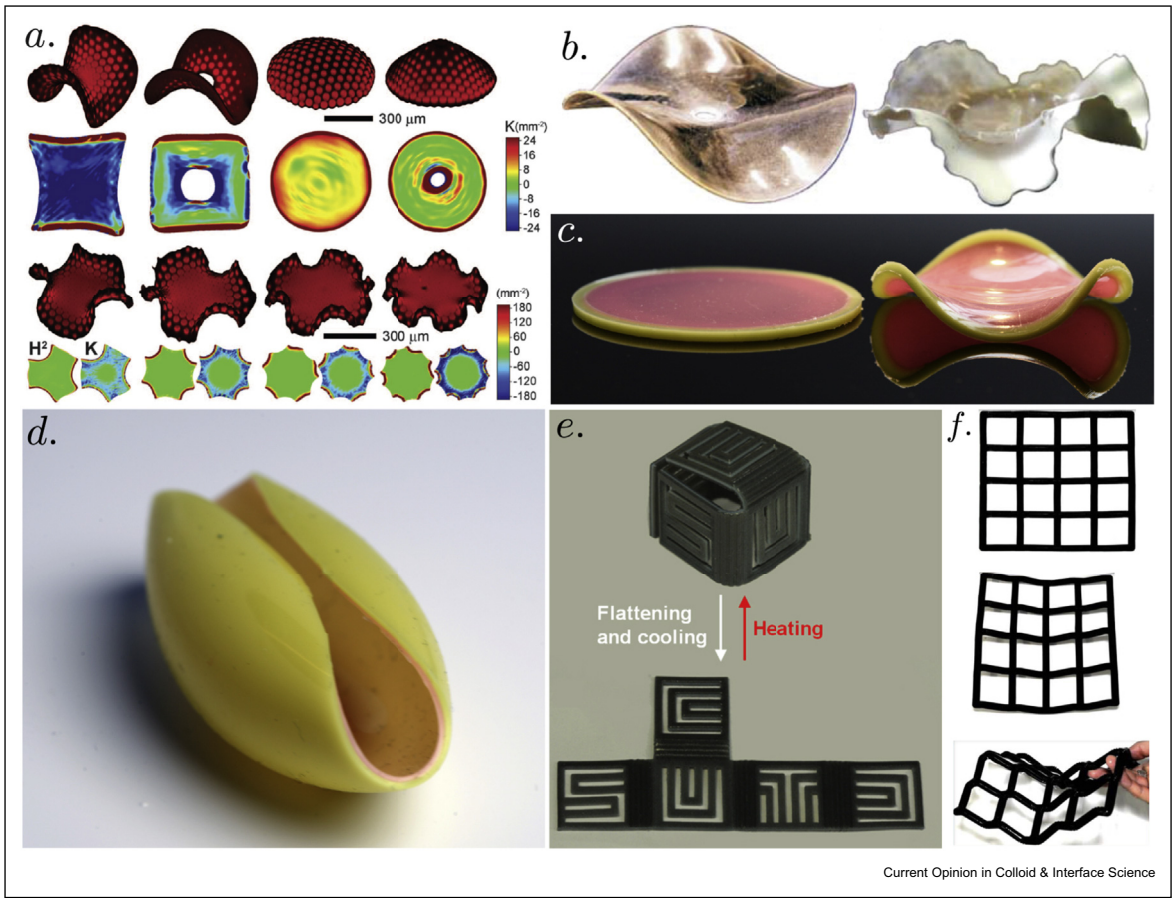

Shape-shifting structures. **(a)** Morphing with halftone lithography adapted from the study by Kim et al. [248]. **(b)** Non-Euclidean plates adapted from the study by Klein et al. [249]. **(c)** A monkey saddle, adapted from the studies by Holmes [250] and Stein-Montalvo et al. [251]. **(d)** Pollen grain isometry of a spherical cap, related to the work in the study by Pezzulla et al. [12]. **(e)** 4D printing using shape–memory polymer joints, adapted from the study by Ge et al. [252]. **(f)** Active printed meshes, adapted from the study by Raviv et al. [253].

Another interesting area may lie at the interface between elastic structures and granular or colloidal materials, so-called elastogranular interactions. Research in this regard is beginning to lay out the fundamental behavior of bending and packing of elastic rods within grains [295–297], which is clearly relevant in the form and function of growing plant roots, an effort that has been led by Prof. Kolb [298–300]. Elastogranular mechanics is beginning to show promise for programmable, reversible architecture [301–303]. Finally, in my opinion, the biggest limitation in achieving the next generation of shape-shifting structures is the absence of simple-to-fabricate and robust materials that are highly responsive to stimuli — that is, we need help from chemists and materials scientists. Dielectric elastomers offer a lot of promise yet require extreme voltages and fail often. Swelling of elastomers and gels is slow, requires a bath of fluid, and usually involves brittle materials that fail when they either deform too much or dry out. We need addressable and programmable materials to take full advantage of the recent advances in mechanical metamaterials. Too often, the research covered in this review uses ordinary office paper, dental polymers, and traditional acrylic plastics and urethane rubbers. This approach is fine and should even be applauded, when the purpose is to show how an appropriate understanding of mechanics, geometry, and topology can make profound predictions with run-of-the-mill materials, but additional materials science advances are necessary to fully realize the potential opportunities for technological insertion of shape-shifting materials. Among the leaders of this effort to connect materials and mechanics is the work of Prof. Sottos et al., who has made advances in self-healing and autonomous damage indicating materials [304–306], and Prof. Hayward et al., see who often works at the interface of polymer chemistry and mechanics [307–309]. Another recent interesting effort to tune the material response of traditional thermal bimorphs highlights the ability to use encapsulated phase change materials to

spontaneously induce thermal bending at critical temperatures [310]. There is much work to be done to better blend the insights from mechanics with the advances in materials.

Conflict of interest statement

Nothing declared.

Acknowledgements

I gratefully acknowledges the financial support from NSF CMMI – CAREER through Mechanics of Materials and Structures (#1454153). I am grateful to L. Stein–Montalvo and X. Jiang for photos and I would like to thank M.A. Dias for many discussions on this topic over the years, and D. Vella for his helpful and insightful comments on the paper. I also thank the organizers of the Kavli Institute for Theoretical Physics (NSF PHY-1748958) program on Geometry, Elasticity, Fluctuations, and Order in 2D Soft Matter for providing me an opportunity to think through some of the ideas detailed within this article. I apologize if I did not cite your work in this review, it was an accident and an oversight on my part, don't @ me.

Appendix A. Supplementary data

Supplementary data to this article can be found online at https://doi.org/10.1016/j.cocis.2019.02.008.

References

Papers of particular interest, published within the period of review, have been highlighted as:

* of special interest
** of outstanding interest

1. Holmes DP: **Supplementary information: elasticity and stability of shape changing structures**. *Curr Opin Colloid Interface Sci* 2019.

2. Sun J-Y, Zhao X, Illeperuma WR, Chaudhuri O, Oh KH, Mooney DJ, Vlassak JJ, Suo Z: **Highly stretchable and tough hydrogels**. *Nature* 2012, **489**:133.

3. Brunck V, Lechenault F, Reid A, Adda-Bedia M: **Elastic theory of origami-based metamaterials**. *Phys Rev* 2016, **93**. 033005.

4. Blees MK, Barnard AW, Rose PA, Roberts SP, McGill KL, Huang PY, Ruyack AR, Kevek JW, Kobrin B, Muller DA, McEuen PL: **Graphene kirigami**. *Nature* 2015, **524**:204.

5. Liu J, Gu T, Shan S, Kang SH, Weaver JC, Bertoldi K: **Harnessing buckling to design architected materials that exhibit effective negative swelling**. *Adv Mater* 2016, **28**: 6619–6624.

6. * Py C, Reverdy P, Doppler L, Bico J, Roman B, Baroud CN: **Capillary origami: spontaneous wrapping of a droplet with an elastic sheet**. *Phys Rev Lett* 2007, **98**:156103.
This paper captured the imagination of many by showing how capillarity can shape thin sheets.

7. Leong TG, Randall CL, Benson BR, Bassik N, Stern GM, Gracias DH: *Tetherless thermobiochemically actuated microgrippers*. Proceedings of the National Academy of Sciences; 2009. pnas–0807698106.

8. Dudte LH, Vouga E, Tachi T, Mahadevan L: **Programming curvature using origami tessellations**. *Nat Mater* 2016, **15**: 583.

9. Pandey A, Moulton D, Vella D, Holmes D: **Dynamics of snapping beams and jumping poppers**. *EPL (Europhysics Lett)* 2014, **105**:24001.

10. Shan S, Kang SH, Raney JR, Wang P, Fang L, Candido F, Lewis JA, Bertoldi K: **Multistable architected materials for trapping elastic strain energy**. *Adv Mater* 2015, **27**:4296–4301.

11. Yang Y, Dias MA, Holmes DP: **Multistable kirigami for tunable architected materials**. *Phys Rev Mater* 2018, **2**:110601.

12. * Pezzulla M, Stoop N, Steranka MP, Bade AJ, Holmes DP: **Curvature-induced instabilities of shells**. *Phys Rev Lett* 2018, **120**. 048002.
Personal bias aside, this paper presents an intuitive mechanical interpretation of an evolving natural curvature stimulus.

13. Rogers JA, Someya T, Huang Y: **Materials and mechanics for stretchable electronics**. *Science* 2010, **327**:1603–1607.

14. Bertoldi K, Reis PM, Willshaw S, Mullin T: **Negative Poisson's ratio behavior induced by an elastic instability**. *Adv Mater* 2010, **22**:361–366.

15. * Cai S, Breid D, Crosby AJ, Suo Z, Hutchinson JW: **Periodic patterns and energy states of buckled films on compliant substrates**. *J Mech Phys Solid* 2011, **59**:1094–1114.
A clear and complete presentation of how wrinkles select their patterns.

16. Rafsanjani A, Bertoldi K: **Buckling-induced kirigami**. *Phys Rev Lett* 2017, **118**. 084301.

17. Föppl A. *Vorlesungen über technische Mechanik*, vol. 5; 1907. Leipzig.

18. Wang C: **A critical review of the heavy elastica**. *Int J Mech Sci* 1986, **28**:549–559.

19. Milner S, Joanny J, Pincus P: **Buckling of Langmuir monolayers**. *EPL (Europhysics Lett)* 1989, **9**:495.

20. Reis PM, Hure J, Jung S, Bush JW, Clanet C: **Grabbing water**. *Soft Matter* 2010, **6**:5705–5708.

21. Callan-Jones A, Brun P-T, Audoly B: **Self-similar curling of a naturally curved elastica**. *Phys Rev Lett* 2012, **108**:174302.

22. Lazarus A, Miller JT, Metlitz MM, Reis PM: **Contorting a heavy and naturally curved elastic rod**. *Soft Matter* 2013, **9**: 8274–8281.

23. Lister JR, Peng GG, Neufeld JA: **Viscous control of peeling an elastic sheet by bending and pulling**. *Phys Rev Lett* 2013, **111**: 154501.

24. Bense H, Trejo M, Reyssat E, Bico J, Roman B: **Buckling of elastomer sheets under non-uniform electro-actuation**. *Soft Matter* 2017, **13**:2876–2885.

25. Pineirua M, Tanaka N, Roman B, Bico J: **Capillary buckling of a floating annulus**. *Soft Matter* 2013, **9**:10985–10992.

26. Audoly B, Pomeau Y: *Elasticity and geometry*. Oxford University Press; 2010.

27. Miller J, Lazarus A, Audoly B, Reis PM: **Shapes of a suspended curly hair**. *Phys Rev Lett* 2014, **112**, 068103.

28. Holmes DP, Borum AD, Moore BF, Plaut RH, Dillard DA: **Equilibria and instabilities of a slinky: discrete model**. *Int J Non-Linear Mech* 2014, **65**:236–244.

29. Argentina M, Mahadevan L: **Fluid-flow-induced flutter of a flag**. *Proc Natl Acad Sci Unit States Am* 2005, **102**:1829–1834.

30. ** Roman B, Bico J: **Elasto-capillarity: deforming an elastic structure with a liquid droplet**. *J Phys Condens Matter* 2010, **22**:493101.
Pioneers of elastocapillary research discussing the topic in great detail and clarity. One can do no better.

31. Bico J, Reyssat É, Roman B: **Elastocapillarity: when surface tension deforms elastic solids**. *Annu Rev Fluid Mech* 2018, **50**: 629–659.

32. Bico J, Roman B, Moulin L, Boudaoud A: **Adhesion: elastocapillary coalescence in wet hair**. *Nature* 2004, **432**:690.

33. * Zhao M, Dervaux J, Narita T, Lequeux F, Limat L, Roché M: **Geometrical control of dissipation during the spreading of liquids on soft solids**. *Proc Natl Acad Sci Unit States Am* 2018, **115**:1748–1753.
A consistent and convincing account of how liquids spread on soft materials, perhaps putting to rest a hotly debated topic.

34. Style RW, Jagota A, Hui C-Y, Dufresne ER: **Elastocapillarity: surface tension and the mechanics of soft solids**. *Annual Rev Condens Matter Physics* 2017, **8**:99–118.

35. Duprat C, Shore HA: *Fluid-structure interactions in low-Reynolds-number flows*. Royal Society of Chemistry; 2015.

36. Crane NB, Onen O, Carballo J, Ni Q, Guldiken R: **Fluidic assembly at the microscale: progress and prospects**. *Microfluid Nanofluidics* 2013, **14**:383–419.

37. Timoshenko S: **Analysis of bi-metal thermostats**. *J Opt Soc Am* 1925, **11**(3):233–255, https://doi.org/10.1364/JOSA.11.000233.

38. Stoney GG: **The tension of metallic films deposited by electrolysis**. *Proc Roy Soc Lond A* 1909, **82**:172–175.

39. Freund LB, Floro JA, Chason E: **Extensions of the Stoney formula for substrate curvature to configurations with thin substrates or large deformations**. *Appl Phys Lett* 1999, **74**:1987.

40. Seffen K, McMahon R: **Heating of a uniform wafer disk**. *Int J Mech Sci* 2007, **49**:230–238.

41. Pezzulla M, Smith GP, Nardinocchi P, Holmes DP: **Geometry and mechanics of thin growing bilayers**. *Soft Matter* 2016, **12**:4435–4442.

42. Bellow DG, Ford G, Kennedy JS: **Anticlastic behavior of flat plates**. *Exp Mech* 1965, **5**:227–232.

43. Pomeroy RJ: **The effect of anticlastic bending on the curvature of beams**. *Int J Solids Struct* 1970, **6**:277–285.

44. Taffetani M, Jiang X, Holmes DP, Vella D: **Static bistability of spherical caps**. *Proc R Soc A* 2018, **474**:20170910.

45. ** Brau F, Vandeparre H, Sabbah A, Poulard C, Boudaoud A, Damman P: **Multiple-length-scale elastic instability mimics parametric resonance of nonlinear oscillators**. *Nat Phys* 2011, **7**:56.

I vividly remember when this paper was published. So elegant and rich. It's findings are still relevant and fundamental to our understanding of elastic instabilities.

46. ** Lazarus A, Florijn H, Reis P: **Geometry-induced rigidity in nonspherical pressurized elastic shells**. *Phys Rev Lett* 2012, **109**:144301.

An everyday occurrence - the rigidity of an egg shell - explained carefully and cleanly in terms of the geometry of curved surfaces.

47. Brinkmeyer A, Santer M, Pirrera A, Weaver P: **Pseudo-bistable self-actuated domes for morphing applications**. *Int J Solids Struct* 2012, **49**:1077–1087.

48. Cerda E, Ravi-Chandar K, Mahadevan L: **Thin films: wrinkling of an elastic sheet under tension**. *Nature* 2002, **419**:579.

49. Cerda E, Mahadevan L: **Geometry and physics of wrinkling**. *Phys Rev Lett* 2003, **90**. 074302.

50. Efimenko K, Rackaitis M, Manias E, Vaziri A, Mahadevan L, Genzer J: **Nested self-similar wrinkling patterns in skins**. *Nat Mater* 2005, **4**:293.

51. Huang J, Juszkiewicz M, De Jeu WH, Cerda E, Emrick T, Menon N, Russell TP: **Capillary wrinkling of floating thin polymer films**. *Science* 2007, **317**:650–653.

52. Allen HG: *Analysis and design of structural sandwich panels*. New York: Pergemon; 1969.

53. Li B, Cao Y-P, Feng X-Q, Gao H: **Mechanics of morphological instabilities and surface wrinkling in soft materials: a review**. *Soft Matter* 2012, **8**:5728–5745.

54. Dillard DA, Mukherjee B, Karnal P, Batra RC, Frechette J: **A review of winkler's foundation and its profound influence on adhesion and soft matter applications**. *Soft Matter* 2018, **14**:3669–3683.

55. Davidovitch B, Schroll RD, Cerda E: **Nonperturbative model for wrinkling in highly bendable sheets**. *Phys Rev* 2012, **85**, https://doi.org/10.1103/PhysRevE.85.066115. 066115.

56. Paulsen JD: **Wrapping liquids, solids, and gases in thin sheets**. *Annual Rev Condens Matter Physics* 2018, **10**:431–450.

57. Vella D, Adda-Bedia M, Cerda E: **Capillary wrinkling of elastic membranes**. *Soft Matter* 2010, **6**:5778.

58. Huang J, Davidovitch B, Santangelo CD, Russell TP, Menon N: **Smooth cascade of wrinkles at the edge of a floating elastic film**. *Phys Rev Lett* 2010, **105**. 038302.

59. Davidovitch B, Schroll RD, Vella D, Adda-Bedia M, Cerda EA: **Prototypical model for tensional wrinkling in thin sheets**. *Proc Natl Academy of Sciences of the United States A* 2011, **108**:18227–18232, https://doi.org/10.1073/pnas.1108553108.

60. * Schroll RD, Adda-Bedia M, Cerda E, Huang J, Menon N, Russell TP, Toga KB, Vella D, Davidovitch B: **Capillary deformations of bendable films**. *Phys Rev Lett* 2013, **111**. 014301.

Over the last decade, these authors have devoted an important and commendable effort to explain the wrinkle to fold transition in floating thin sheets.

61. Vella D, Davidovitch B: **Regimes of wrinkling in an indented floating elastic sheet**. *Phys Rev E* 2018, **98**:013003.

62. Taffetani M, Vella D: **Regimes of wrinkling in pressurized elastic shells**. *Phil Trans R Soc A* 2017, **375**:20160330.

63. Holmes DP, Crosby AJ: **Draping films: a wrinkle to fold transition**. *Phys Rev Lett* 2010, **105**. 038303.

64. Vella D, Ajdari A, Vaziri A, Boudaoud A: **The indentation of pressurized elastic shells: from polymeric capsules to yeast cells**. *J R Soc Interface* 2012, **9**:448–455.

65. Vella D, Ajdari A, Vaziri A, Boudaoud A: **Indentation of ellipsoidal and cylindrical elastic shells**. *Phys Rev Lett* 2012, **109**:144302.

66. Vella D, Ajdari A, Vaziri A, Boudaoud A: **Wrinkling of pressurized elastic shells**. *Phys Rev Lett* 2011, **107**:174301.

67. Milani P, Braybrook SA, Boudaoud A: **Shrinking the hammer: micromechanical approaches to morphogenesis**. *J Exp Bot* 2013, **64**:4651–4662.

68. Minc N, Boudaoud A, Chang F: **Mechanical forces of fission yeast growth**. *Curr Biol* 2009, **19**:1096–1101.

69. Zdunek A, Kurenda A: **Determination of the elastic properties of tomato fruit cells with an atomic force microscope**. *Sensors* 2013, **13**:12175–12191.

70. Routier-Kierzkowska A-L, Smith RS: **Measuring the mechanics of morphogenesis**. *Curr Opin Plant Biol* 2013, **16**:25–32.

71. Robinson S, Burian A, Couturier E, Landrein B, Louveaux M, Neumann ED, Peaucelle A, Weber A, Nakayama N: **Mechanical control of morphogenesis at the shoot apex**. *J Exp Bot* 2013, **64**:4729–4744. ert199.

72. Neubauer MP, Poehlmann M, Fery A: **Microcapsule mechanics: from stability to function**. *Adv Colloid Interface Sci* 2014, **207**:65–80.

73. Goriely A. *The mathematics and mechanics of biological growth*, vol. 45. Springer; 2017.

74. Groenewold J: **Wrinkling of plates coupled with soft elastic media**. *Physica A* 2001, **298**:32–45.

75. Kücken M, Newell A: **Fingerprint formation**. *J Theor Biol* 2005, **235**:71–83.

76. ** Goriely A, Geers MG, Holzapfel GA, Jayamohan J, Jérusalem A, Sivaloganathan S, Squier W, van Dommelen JA, Waters S, Kuhl E: **Mechanics of the brain: perspectives, challenges, and opportunities**. *Biomechanics Model Mechanobiol* 2015, **14**:931–965.

The role of mechanics vs. biology in the growth and development of the brain was a long debated topic. Goriely and Kuhl go above and beyond to provide clarity on the subject.

77. Budday S, Steinmann P, Goriely A, Kuhl E: **Size and curvature regulate pattern selection in the mammalian brain**. *Extr Mech Lett* 2015, **4**:193–198.

78. Tallinen T, Chung JY, Rousseau F, Girard N, Lefèvre J, Mahadevan L: **On the growth and form of cortical convolutions**. *Nat Phys* 2016, **12**:588.

79. Goriely A, Tabor M: **Spontaneous helix hand reversal and tendril perversion in climbing plants**. *Phys Rev Lett* 1998, **80**: 1564.

80. Feynman RP, Leighton RB, Sands M. *The feynman lectures on physics: mainly electromagnetism and matter*, vol. 2. Addison-Wesley, Reading. reprinted; 1977. Ch. 19.

81. Budiansky B: *Buckling of structures: symposium cambridge/USA, june 17–21, 1974*. Springer Science & Business Media; 2013.

82. Thompson JMT, Hunt GW: *A general theory of elastic stability*. London: J. Wiley; 1973.

83. Thompson JMT, Hunt GW. *Elastic instability phenomena*, vol. 2. Wiley Chichester; 1984.

84. Kosterlitz JM, Thouless DJ: **Ordering, metastability and phase transitions in two-dimensional systems**. *J Phys C Solid State Phys* 1973, **6**:1181.

85. Mikulinsky M, Livshits D: **Pre-and postbuckling behavior of mechanical structures in terms of phase transitions**. *Int J Eng Sci* 1995, **33**:1987–2000.

86. * Savelev S, Nori F: **Magnetic and mechanical buckling: modified landau theory approach to study phase transitions in micromagnetic disks and compressed rods**. *Phys Rev B* 2004, **70**:214415.
Lovely use of Landau's theory of phase transitions to a buckling problem.

87. Hu N, Burgueño R: **Buckling-induced smart applications: recent advances and trends**. *Smart Mater Struct* 2015, **24**: 1–21.

88. Jakomin MR, Kosel F, Kosel T: **Thin double curved shallow bimetallic shell in a homogeneous temperature field by nonlinear theory**. *Thin-Walled Struct* 2010, **48**:243–259.

89. Shankar MR, Smith ML, Tondiglia VP, Lee KM, McConney ME, Wang DH, Tan L-S, White TJ: **Contactless, photoinitiated snap-through in azobenzene-functionalized polymers**. *Proc Natl Acad Sci Unit States Am* 2013, **110**:18792–18797.

90. Ng C: **Nonlinear and snap-through responses of curved panels to intense acoustic excitation**. *J Aircraft* 1989, **26**: 281–288.

91. Murphy K, Virgin L, Rizzi S: **Experimental snap-through boundaries for acoustically excited, thermally buckled plates**. *Exp Mech* 1996, **36**:312–317.

92. Holmes DP, Crosby AJ: **Snapping surfaces**. *Adv Matter* 2007, **19**:3589–3593.

93. Xia C, Lee H, Fang N: **Solvent-driven polymeric micro beam device**. *J Micromech Microeng* 2010, **20**. 085030.

94. Abdullah AM, Braun PV, Hsia KJ: **Programmable shape transformation of elastic spherical domes**. *Soft Matter* 2016, **12**: 6184–6195.

95. Zhu Y, Zu JW: **Enhanced buckled-beam piezoelectric energy harvesting using midpoint magnetic force**. *Appl Phys Lett* 2013, **103**. 041905.

96. Seffen KA, Vidoli S: **Eversion of bistable shells under magnetic actuation: a model of nonlinear shapes**. *Smart Mater Struct* 2016, **25**. 065010.

97. Gomez M, Moulton DE, Vella D: **Passive control of viscous flow via elastic snap-through**. *Phys Rev Lett* 2017, **119**:144502.

98. Fargette A, Neukirch S, Antkowiak A: **Elastocapillary snapping: capillarity induces snap-through instabilities in small elastic beams**. *Phys Rev Lett* 2014, **112**:137802.

99. Schultz MR, Hyer MW: **Snap-through of unsymmetric cross-ply laminates using piezoceramic actuators**. *J Intell Mater Syst Struct* 2003, **14**:795–814.

100. Giannopoulos G, Monreal J, Vantomme J: **Snap-through buckling behavior of piezoelectric bimorph beams: I. Analytical and numerical modeling**. *Smart Mater Struct* 2007, **16**: 1148–1157.

101. Zhang Y, Wang Y, Li Z, Huang Y, Li D: **Snap-through and pull-in instabilities of an arch-shaped beam under an electrostatic loading**. *Journal of Microelectromechanical Systems* 2007, **16**: 684–693.

102. Krylov S, Ilic BR, Lulinsky S: **Bistability of curved microbeams actuated by fringing electrostatic fields**. *Nonlinear Dynam* 2011, **66**:403.

103. Keplinger C, Li T, Baumgartner R, Suo Z, Bauer S: **Harnessing snap-through instability in soft dielectrics to achieve giant voltage-triggered deformation**. *Soft Matter* 2011, **8**:285.

104. Zhao X, Wang Q: **Harnessing large deformation and instabilities of soft dielectrics: theory, experiment, and application**. *Appl Phys Rev* 2014, **1**. 021304.

105. Shao H, Wei S, Jiang X, Holmes DP, Ghosh TK: **Bioinspired electrically activated soft bistable actuators**. *Adv Funct Mater* 2018:1802999.

106. Hufenbach W, Gude M, Kroll L: **Design of multistable composites for application in adaptive structures**. *Compos Sci Technol* 2002, **62**:2201–2207.

107. Lachenal X, Weaver PM, Daynes S: **Multi-stable composite twisting structure for morphing applications**. *Proc Math Phys Eng Sci* 2012, **468**:1230–1251.

108. Zhang Z, Wu H, He X, Wu H, Bao Y, Chai G: **The bistable behaviors of carbon-fiber/epoxy anti-symmetric composite shells**. *Compos B Eng* 2013, **47**:190–199.

109. Ryu J, Lee J-G, Kim S-W, Koh J-S, Cho K-J, Cho M: **Generalized curvature tailoring of bistable cfrp laminates by curing on a cylindrical tool-plate with misalignment**. *Compos Sci Technol* 2014, **103**:127–133.

110. Lachenal X, Daynes S, Weaver PM: **Review of morphing concepts and materials for wind turbine blade applications**. *Wind Energy* 2013, **16**:283–307.

111. Lienhard J, Schleicher S, Poppinga S, Masselter T, Milwich M, Speck T, Knippers J: **Flectofin: a hingeless flapping mechanism inspired by nature**. *Bioinspiration Biomimetics* 2011, **6**. 045001.

112. Gonçalves P: **Dynamic non-linear behavior and stability of a ventricular assist device**. *Int J Solids Struct* 2003, **40**: 5017–5035.

113. * Seffen KA, Pellegrino S: **Deployment dynamics of tape springs**. *Proc Roy Soc Lond: Math Phy Eng Sci* 1999, **455**:1003–1048.
A thorough examination of deployable tape springs, or `snap bracelets.

114. Walker S, Aglietti GS: **A study of tape spring fold curvature for space deployable structures**. *Proc IME G J Aero Eng* 2007, **221**(3):313–325.

115. Kebadze E, Guest S, Pellegrino S: **Bistable prestressed shell structures**. *Int J Solids Struct* 2004, **41**:2801–2820.

116. Chen Z, Guo Q, Majidi C, Chen W, Srolovitz DJ, Haataja MP: **Nonlinear geometric effects in mechanical bistable morphing structures**. *Phys Rev Lett* 2012, **109**:114302.

117. Jiang X, Pezzulla M, Shao H, Ghosh TK, Holmes DP: **Snapping of bistable, prestressed cylindrical shells**. *Europhys Lett* 2018, **122**:64003.

118. * Lee A, Brun P-T, Marthelot J, Balestra G, Gallaire F, Reis P: **Fabrication of slender elastic shells by the coating of curved surfaces**. *Nat Commun* 2016, **7**:11155.
A beautifully simple way to prepare thin elastic shells. Can be adapted to cylinders and cones without much trouble.

119. Li T, Zhang Z: **Snap-through instability of graphene on substrates**. *Nanoscale Res Lett* 2009, **5**:169–173.

120. Scharfenberg S, Mansukhani N, Chialvo C, Weaver RL, Mason N: **Observation of a snap-through instability in graphene**. *Appl Phys Lett* 2012, **100**. 021910.

121. Lindahl N, Midtvedt D, Svensson J, Nerushev OA, Lindvall N, Isacsson A, Campbell EE: **Determination of the bending rigidity of graphene via electrostatic actuation of buckled membranes**. *Nano Lett* 2012, **12**:3526–3531.

122. Jaglinski T, Kochmann D, Stone D, Lakes R: **Composite materials with viscoelastic stiffness greater than diamond**. *Science* 2007, **315**:620–622.

123. Hsu C, Hsu W: **Instability in micromachined curved thermal bimorph structures**. *J Micromech Microeng* 2003, **13**:955–962.

124. Hansen BJ, Carron CJ, Jensen B, Hawkins A, Schultz S: **Plastic latching accelerometer based on bistable compliant mechanisms**. *Smart Mater Struct* 2007, **16**:1967.

125. Hanna BH, Lund JM, Lang RJ, Magleby SP, Howell LL: **Waterbomb base: a symmetric single-vertex bistable origami mechanism**. *Smart Mater Struct* 2014, **23**. 094009.

126. Bowen L, Springsteen K, Feldstein H, Frecker M, Simpson TW, von Lockette P: **Development and validation of a dynamic model of magneto-active elastomer actuation of the origami waterbomb base**. *J Mech Robot* 2015, **7**. 011010.

127. Chen Y, Feng H, Ma J, Peng R, You Z: **Symmetric waterbomb origami**. *Proc R Soc A* 2016, **472**:20150846.

128. Bende NP, Evans AA, Innes-Gold S, Marin LA, Cohen I, Hayward RC, Santangelo CD: **Geometrically controlled snapping transitions in shells with curved creases**. *Proc Natl Acad Sci Unit States Am* 2015, **112**:11175–11180.

129. Pellegrini SP, Tolou N, Schenk M, Herder JL: **Bistable vibration energy harvesters: a review**. *J Intell Mater Syst Struct* 2013, **24**:1303–1312.

130. Raney JR, Nadkarni N, Daraio C, Kochmann DM, Lewis JA, Bertoldi K: *Stable propagation of mechanical signals in soft media using stored elastic energy*. Proceedings of the National Academy of Sciences; 2016:201604838.

131. Li B, Liu L, Suo Z: **Extension limit, polarization saturation, and snap-through instability of dielectric elastomers**. *Int J Soc Netw Min* 2011, **2**:59–67.

132. * Overvelde JT, Kloek T, Dahaen JJ, Bertoldi K: **Amplifying the response of soft actuators by harnessing snap-through instabilities**. *Proc Natl Acad Sci Unit States Am* 2015, **112**:10863–10868.

Excellent demonstration of snap-through instabilities can be utilized by soft materials.

133. Reis PM: **A perspective on the revival of structural (in) stability with novel opportunities for function: from buckliphobia to buckliphilia**. *J Appl Mech* 2015, **82**:111001.

134. Holmes DP, Tavakol B, Froehlicher G, Stone H: **Control and manipulation of microfluidic flow via elastic deformations**. *Soft Matter* 2013, **9**:7049.

135. Tavakol B, Holmes DP: **Voltage-induced buckling of dielectric films using fluid electrodes**. *Appl Phys Lett* 2016, **108**:112901.

136. Someya T, Kato Y, Sekitani T, Iba S, Noguchi Y, Murase Y, Kawaguchi H, Sakurai T: **Conformable, flexible, large-area networks of pressure and thermal sensors with organic transistor active matrixes**. *Proc Natl Acad Sci Unit States Am* 2005, **102**:12321–12325.

137. Sun Y, Choi W, Jiang H, Huang YY, Rogers JA: **Controlled buckling of semiconductor nanoribbons for stretchable electronics**. *Nat Nanotechnol* 2006, **1**:201–207.

138. Lu X, Xia Y: **Electronic materials - buckling down for flexible electronics**. *Nat Nanotechnol* 2006, **1**:163–164.

139. Kim D-H, Rogers JA: **Stretchable electronics: materials strategies and devices**. *Adv Mater* 2008, **20**:4887–4892.

140. Kim D-H, Song J, Choi WM, Kim H-S, Kim R-H, Liu Z, Huang YY, Hwang K-C, Zhang Y-W, Rogers JA: **Materials and noncoplanar mesh designs for integrated circuits with linear elastic responses to extreme mechanical deformations**. *Proc Natl Academy of Sciences of the United States A* 2008, **105**:18675–18680.

141. Khang D-Y, Rogers JA, Lee HH: **Mechanical buckling: mechanics, metrology, and stretchable electronics**. *Adv Funct Mater* 2009, **19**:1526–1536.

142. Khang D-Y, Xiao J, Kocabas C, MacLaren S, Banks T, Jiang H, Huang YY, Rogers JA: **Molecular scale buckling mechanics in individual aligned single-wall carbon nanotubes on elastomeric substrates**. *Nano Lett* 2008, **8**:124–130.

143. Kim DH, Ahn JH, Choi WM, Kim HS, Kim TH, Song J, Huang YY, Liu Z, Lu C, Rogers JA: **Stretchable and foldable silicon integrated circuits**. *Science* 2008, **320**:507–511.

144. Qi Y, Kim J, Nguyen TD, Lisko B, Purohit PK, McAlpine MC: **Enhanced piezoelectricity and stretchability in energy harvesting devices fabricated from buckled PZT ribbons**. *Nano Lett* 2011, **11**:1331–1336.

145. Abdullah AM, Li X, Braun PV, Rogers JA, Hsia KJ: **Self-folded gripper-like architectures from stimuli-responsive bilayers**. *Adv Mater* 2018:1801669.

146. * Knoche S, Kierfeld J: **Buckling of spherical capsules**. *Phys Rev* 2011, **84**. 046608.

One of the best modern treatments of buckling shells and colloids.

147. Nasto A, Ajdari A, Lazarus A, Vaziri A, Reis PM: **Localization of deformation in thin shells under indentation**. *Soft Matter* 2013, **9**:699.

148. * Stoop N, Lagrange R, Terwagne D, Reis PM, Dunkel J: **Curvature-induced symmetry breaking determines elastic surface patterns**. *Nat Mater* 2015, **14**:337.

Really nice demonstration of how symmetry breaking can control pattern formation.

149. Jiménez FL, Stoop N, Lagrange R, Dunkel J, Reis PM: **Curvature-controlled defect localization in elastic surface crystals**. *Phys Rev Lett* 2016, **116**:104301.

150. Marthelot J, Brun P-T, Jiménez FL, Reis PM: **Reversible patterning of spherical shells through constrained buckling**. *Phys Rev Mater* 2017, **1**. 025601.

151. Chung JY, Vaziri A, Mahadevan L: *Reprogrammable braille on an elastic shell*. Proceedings of the National Academy of Sciences; 2018:201722342.

152. Terwagne D, Brojan M, Reis PM: **Smart morphable surfaces for aerodynamic drag control**. *Adv Mater* 2014, **26**:6608–6611.

153. Guttag M, Reis PM: **Active aerodynamic drag reduction on morphable cylinders**. *Phy Rev Fluid* 2017, **2**:123903.

154. * Sacanna S, Irvine WTM, Rossi L, Pine DJ: **Lock and key colloids through polymerization-induced buckling of monodisperse silicon oil droplets**. *Soft Matter* 2011, **7**:1631–1634.

I remember being blown away by the creativity of this research when I first saw it. I believe there is still a significant opportunity for rich science in this area of buckling colloids.

155. Jampani VSR, Mulder DJ, De Sousa KR, Gélébart A-H, Lagerwall JP, Schenning AP: **Micrometer-scale porous buckling shell actuators based on liquid crystal networks**. *Adv Funct Mater* 2018:1801209.

156. * Djellouli A, Marmottant P, Djeridi H, Quilliet C, Coupier G: **Buckling instability causes inertial thrust for spherical swimmers at all scales**. *Phys Rev Lett* 2017, **119**:224501.

Swimming shells by buckling - brilliant.

157. Bowden N, Brittain S, Evan AG, Hutchinson JW, Whitesides GW: **Spontaneous formation of ordered structures in thin films of metals supported on an elastomeric polymer**. *Nature* 1998, **393**:146–149.

158. Huck WTS, Bowden N, Onck P, Pardoen T, Hutchinson JW, Whitesides GM: **Ordering of spontaneously formed buckles on planar surfaces**. *Langmuir* 2000, **16**:3497–3501.

159. Parfitt GG, Lambeth D: **The damping of structural vibrations**. *Ministry Aviation Aeronautical Res Council Curr Papers* 1962:1–34.

160. Lacour SP, Wagner S, Huang Z, Suo Z: **Stretchable gold conductors on elastomeric substrates**. *Appl Phys Lett* 2003, **82**:2404–2406.

161. Choi WM, Song J, Khang D-Y, Jiang H, Huang YY, Rogers JA: **Biaxially stretchable "wavy" silicon nanomembranes**. *Nano Lett* 2007, **7**:1655–1663.

162. Wang Y, Yang R, Shi Z, Zhang L, Shi D, Wang E, Zhang G: **Super-elastic graphene ripples for flexible strain sensors**. *ACS Nano* 2011, **5**:3645–3650.

163. Yu C, Masarapu C, Rong J, Wei B, Jiang H: **Stretchable supercapacitors based on buckled single-walled carbon-nanotube macrofilms**. *Adv Mater* 2009, **21**:4793–4797.

164. Rand CJ, Crosby AJ: **Friction of soft elastomeric wrinkled surfaces**. *J Appl Phys* 2009, **106**. 064913.

165. Suzuki K, Hirai Y, Ohzono T: **Oscillating friction on shape-tunable wrinkles**. *ACS Appl Mater Interfaces* 2014, **6**: 10121–10131.

166. Harrison C, Stafford CM, Zhang W, Karim A: **Sinusoidal phase grating created by a tunably buckled surface**. *Appl Phys Lett* 2004, **85**:4016.

167. Stafford CM, Harrison C, Beers KL, Karim A, Amis EJ, VanLandingham MR, Kim H-C, Volksen W, Miller RD, Simonyi EE: **A buckling-based metrology for measuring the elastic moduli of polymeric thin films**. *Nat Mater* 2004, **3**: 545–550.

168. Autumn K, Peattie AM: **Mechanisms of adhesion in geckos**. In *Integrative and comparative biology*; 2002:1081–1090.

169. Chan E, Greiner C, Arzt E, Crosby AJ: **Designing model systems for enhanced adhesion**. *MRS Bull* 2007, **32**: 496–503.

170. Davis CS, Crosby AJ: **Mechanics of wrinkled surface adhesion**. *Soft Matter* 2011, **7**:5373.

171. Davis CS, Martina D, Creton C, Lindner A, Crosby AJ: **Enhanced adhesion of elastic materials to small-scale wrinkles**. *Langmuir* 2012, **28**:14899–14908.

172. Chopin J, Kudrolli A: **Helicoids, wrinkles, and loops in twisted ribbons**. *Phys Rev Lett* 2013, **111**:174302.

173. Kudrolli A, Chopin J: **Tension-dependent transverse buckles and wrinkles in twisted elastic sheets**. *Proc R Soc A* 2018, **474**:20180062.

174. Chen X, Hutchinson JW: **Herringbone buckling patterns of compressed thin films on compliant substrates**. *J Appl Mech* 2004, **71**:597–603.

175. Audoly B, Boudaoud A: **Buckling of a stiff film bound to a compliant substrate part i:** *J Mech Phys Solid* 2008, **56**: 2401–2421, https://doi.org/10.1016/j.jmps.2008.03.003.
** If you are interested in the mechanics behind wrinkling you can do no better than this three-part paper - challenging yet rewarding.

176. Pocivavsek L, Dellsy R, Kern A, Johnson S, Lin B, Lee KYC, Cerda E: **Stress and fold localization in thin elastic membranes**. *Science* 2008, **320**:912–916.
* This is the first paper I read that examined the wrinkle to fold transition in thin films. Its early contributions are still important to the field.

177. Shim J, Perdigou C, Chen ER, Bertoldi K, Reis PM: **Buckling-induced encapsulation of structured elastic shells under pressure**. *Proc Natl Acad Sci* 2012, **109**:5978–5983.

178. Coulais C, Sounas D, Alù A: **Static non-reciprocity in mechanical metamaterials**. *Nature* 2017, **542**:461.

179. Coulais C, Teomy E, de Reus K, Shokef Y, van Hecke M: **Combinatorial design of textured mechanical metamaterials**. *Nature* 2016, **535**:529–532.

180. Florijn B, Coulais C, van Hecke M: **Programmable mechanical metamaterials**. *Phys Rev Lett* 2014, **113**:175503.

181. Kadic M, Bückmann T, Schittny R, Wegener M: **Metamaterials beyond electromagnetism**. *Rep Prog Phys* 2013, **76**:126501.
* If you have any interest in metamaterials, start here.

182. Bertoldi K, Vitelli V, Christensen J, van Hecke M: **Flexible mechanical metamaterials**. *Nature Rev Mater* 2017, **2**:17066.

183. Lakes R: **Foam structures with a negative Poisson's ratio**. *Science* 1987:1038–1040.

184. Grima JN, Evans KE: **Auxetic behavior from rotating squares**. *J Mater Sci Lett* 2000, **19**:1563–1565.

185. Mullin T, Deschanel S, Bertoldi K, Boyce MC: **Pattern transformation triggered by deformation**. *Phys Rev Lett* 2007, **99**. 084301.

186. Florijn B, Coulais C, van Hecke M: **Programmable mechanical metamaterials: the role of geometry**. *Soft Matter* 2016, **12**: 8736–8743.

187. Nicolaou ZG, Motter AE: **Mechanical metamaterials with negative compressibility transitions**. *Nat Mater* 2012, **11**:608.

188. Coulais C, Overvelde JT, Lubbers LA, Bertoldi K, van Hecke M: **Discontinuous buckling of wide beams and metabeams**. *Phys Rev Lett* 2015, **115**. 044301.

189. Coulais C, Kettenis C, van Hecke M: **A characteristic length scale causes anomalous size effects and boundary programmability in mechanical metamaterials**. *Nat Phys* 2018, **14**:40.

190. Rocklin DZ, Zhou S, Sun K, Mao X: **Transformable topological mechanical metamaterials**. *Nat Commun* 2017, **8**:14201.

191. Witten T: **Stress focusing in elastic sheets**. *Rev Mod Phys* 2007, **79**:643–675, https://doi.org/10.1103/RevModPhys.79.643.
** This paper had an enormous affect on me as a student. At the time, I had no idea that the study of crumpled paper could be so rich and confounding and complex. This review provided a roadmap forward.

192. Engel H, Engel H, Architect G: *Structure systems*. Van Nostrand Reinhold Company; 1981.

193. Pellegrino S: *Deployable structures*. Springer; 2001.

194. Cipra BA: **In the fold: origami meets mathematics**. *SIAM News* 2001, **34**:1–4.

195. Klett Y, Drechsler K: **Designing technical tessellations**. *Origami* 2011, **5**:305–322.

196. Peraza-Hernandez EA, Hartl DJ, Malak Jr RJ, Lagoudas DC: **Origami-inspired active structures: a synthesis and review**. *Smart Mater Struct* 2014, **23**. 094001.

197. Lechenault F, Thiria B, Adda-Bedia M: **Mechanical response of a creased sheet**. *Phys Rev Lett* 2014, **112**:244301.

198. Farmer SM, Calladine CR: **Geometry of 'developable cones'**. *Int J Mech Sci* 2005, **47**:509–520.

199. Müller MM, Amar MB, Guven J: **Conical defects in growing sheets**. *Phys Rev Lett* 2008, **101**:156104.

200. Guven J, Hanna J, Kahraman O, Müller MM: **Dipoles in thin sheets**. *European Phys J E* 2013, **36**:106.
* An elegant examination of defects, or dipoles, in sheets and their interactions.

201. Seffen KA: **Fundamental conical defects: the d-cone, its e-cone, and its p-cone**. *Phys Rev* 2016, vol. 94. 013002.

202. Croll AB, Twohig T, Elder T: **The compressive strength of crumpled matter**. *Nat Commun* 2019, **10**:1502.
* While we often focus on geometry, this article is a refreshing reminder of the important role that material properties, specifically how adhesion affects crumpling.

203. Waitukaitis S, van Hecke M: **Origami building blocks: generic and special four-vertices**. *Phys Rev* 2016, **93**. 023003.

204. Silverberg JL, Evans AA, McLeod L, Hayward RC, Hull T, Santangelo CD, Cohen I: **Using origami design principles to fold reprogrammable mechanical metamaterials**. *Science* 2014, **345**:647–650.

205. Filipov ET, Tachi T, Paulino GH: **Origami tubes assembled into stiff, yet reconfigurable structures and metamaterials**. *Proc Natl Acad Sci Unit States Am* 2015, **112**:12321–12326.

206. Overvelde JT, Weaver JC, Hoberman C, Bertoldi K: **Rational design of reconfigurable prismatic architected materials**. *Nature* 2017, **541**:347.

207. Overvelde JT, De Jong TA, Shevchenko Y, Becerra SA, Whitesides GM, Weaver JC, Hoberman C, Bertoldi K: **A three-dimensional actuated origami-inspired transformable metamaterial with multiple degrees of freedom**. *Nat Commun* 2016, **7**:10929.

208. Waitukaitis S, Menaut R, Chen B G-g, van Hecke M: **Origami multistability: from single vertices to metasheets**. *Phys Rev Lett* 2015, **114**. 055503.

Coupling origami and multistability, all resting on an intuitive physical framework.

209. Silverberg JL, Na J-H, Evans AA, Liu B, Hull TC, Santangelo CD, Lang RJ, Hayward RC, Cohen I: **Origami structures with a critical transition to bistability arising from hidden degrees of freedom**. *Nat Mater* 2015, **14**:389.

210. K. Miura, Method of packing and deployment of large membranes in space, The Institute of Space and Astronautical Science.

211. Wei ZY, Guo ZV, Dudte L, Liang HY, Mahadevan L: **Geometric mechanics of periodic pleated origami**. *Phys Rev Lett* 2013, **110**:215501.

212. Schenk M, Guest SD: **Geometry of miura-folded metamaterials**. *Proc Natl Academy of Sciences of the United States A* 2013, **110**:3276–3281, https://doi.org/10.1073/pnas.1217998110.

213. Zirbel SA, Lang RJ, Thomson MW, Sigel DA, Walkemeyer PE, Trease BP, Magleby SP, Howell LL: **Accommodating thickness in origami-based deployable arrays 1**. *J Mech Des* 2013, **135**:111005.

214. Cheng Q, Song Z, Ma T, Smith BB, Tang R, Yu H, Jiang H, Chan CK: **Folding paper-based lithium-ion batteries for higher areal energy densities**. *Nano Lett* 2013, **13**:4969–4974.

215. You Z, Kuribayashi K: *A novel origami stent, 2003 summer bioengineering conference*. 2003:1–2.

216. In HJ, Kumar S, Shao-Horn Y, Barbastathis G: **Origami fabrication of nanostructured, three-dimensional devices: electrochemical capacitors with carbon electrodes**. *Appl Phys Lett* 2006, **88**. 083104.

217. Tremblay EJ, Stack RA, Morrison RL, Ford JE: **Ultrathin cameras using annular folded optics**. *Appl Optic* 2007, **46**(4):463–471.

218. Myers B, Bernardi M, Grossman JC: **Three-dimensional photovoltaics**. *Appl Phys Lett* 2010, **96**. 071902.

219. Elisa B, Nikolaos V, Katia B: **Origami metamaterials for tunable thermal expansion**. *Adv Mater* 2017, **29**:1700360.

220. Wu Y, Lai Y, Zhang Z-Q: **Elastic metamaterials with simultaneously negative effective shear modulus and mass density**. *Phys Rev Lett* 2011, **107**:105506, https://doi.org/10.1103/PhysRevLett.107.105506.

221. Hawkes E, An B, Benbernou NM, Tanaka H, Kim S, Demaine ED, Rus D, Wood RJ: **Programmable matter by folding**. *Proc Natl Acad Sci Unit States Am* 2010, **107**:12441–12445.

222. Ryu J, D'Amato M, Cui X, Long KN, Qi HJ, Dunn ML: **Photo-origami—bending and folding polymers with light**. *Appl Phys Lett* 2012, **100**:161908.

223. Liu Y, Boyles JK, Genzer J, Dickey MD: **Self-folding of polymer sheets using local light absorption**. *Soft Matter* 2012, **8**:1764, https://doi.org/10.1039/c1sm06564e.

224. Liu C, Lopes MC, Pihan SA, Fell D, Sokuler M, Butt H-J, Auernhammer GK, Bonaccurso E: **Water diffusion in polymer nano-films measured with microcantilevers**. *Sensor Actuator B Chem* 2011, **160**:32–38.

225. Ahn BY, Shoji D, Hansen CJ, Hong E, Dunand DC, Lewis JA: **Printed origami structures**. *Adv Mater* 2010, **22**:2251–2254.

226. Moshe M, Shankar S, Bowick MJ, Nelson DR: **Nonlinear mechanics of thin frames**. *Phys Rev E* 2019, **99**:013002.

227. Chen BG-G, Liu B, Evans AA, Paulose J, Cohen I, Vitelli V, Santangelo CD: **Topological mechanics of origami and kirigami**. *Phys Rev Lett* 2016, **116**:135501.

228. * Castle T, Cho Y, Gong X, Jung E, Sussman DM, Yang S, Kamien RD: **Making the cut: lattice kirigami rules**. *Phys Rev Lett* 2014, **113**:245502.
A geometric approach to kirigami that provides building blocks for lattice structures.

229. Sussman DM, Cho Y, Castle T, Gong X, Jung E, Yang S, Kamien RD: **Algorithmic lattice kirigami: a route to pluripotent materials**. *Proc Natl Acad Sci Unit States Am* 2015, **112**:7449.

230. Tang Y, Yin J: **Design of cut unit geometry in hierarchical kirigami-based auxetic metamaterials for high stretchability and compressibility**. *Extr Mech Lett* 2017, **12**:77.

231. Dias MA, McCarron MP, Rayneau-Kirkhope D, Hanakata PZ, Campbell DK, Park HS, Holmes DP: *Kirigami Actuators, Soft Matter* 2017, **13**:9087–9092.

232. Tang Y, Lin G, Yang S, Yi YK, Kamien RD, Yin J: **Programmable kiri-kirigami metamaterials**. *Adv Mater* 2017, **29**:1604262.

233. Grima JN, Mizzi L, Azzopardi KM, Gatt R: **Auxetic perforated mechanical metamaterials with randomly oriented cuts**. *Adv Mater* 2016, **28**:385.

234. Cho Y, Shin J-H, Costa A, Kim TA, Kunin V, Li J, Lee SY, Yang S, Han HN, Choi I-S, Srolovitz DJ: **Engineering the shape and structure of materials by fractal cut**. *Proc Natl Acad Sci Unit States Am* 2014, **111**:17390–17395.

235. Yang S, Choi I-S, Kamien RD: **Design of super-conformable, foldable materials via fractal cuts and lattice kirigami**. *MRS Bull* 2016, **41**:130.

236. Wu C, Wang X, Lin L, Guo H, Wang ZL: **Paper-based triboelectric nanogenerators made of stretchable interlocking kirigami patterns**. *ACS Nano* 2016, **10**:4652–4659.

237. Shyu TC, Damasceno PF, Dodd PM, Lamoureux A, Xu L, Shlian M, Shtein M, Glotzer SC, Kotov NA: **A kirigami approach to engineering elasticity in nanocomposites through patterned defects**. *Nat Mater* 2015, **14**:785.

238. Zhang Y, Yan Z, Nan K, Xiao D, Liu Y, Luan H, Fu H, Wang X, Yang Q, Wang J, Ren W, Si H, Liu F, Yang L, Li H, Wang J, Guo X, Luo H, Wang L, Huang Y, Rogers JA: **A mechanically driven form of kirigami as a route to 3d mesostructures in micro/nanomembranes**. *Proc Natl Acad Sci Unit States Am* 2015, **112**:11757.

239. Tang Y, Lin G, Han L, Qiu S, Yang S, Yin J: **Design of hierarchically cut hinges for highly stretchable and reconfigurable metamaterials with enhanced strength**. *Adv Mater* 2015, **27**:7181–7190.

240. Ou JY, Plum E, Jiang L, Zheludev NI: **Reconfigurable photonic metamaterials**. *Nano Lett* 2011, **11**:2142.

241. Hwang D-G, Bartlett MD: **Tunable mechanical metamaterials through hybrid kirigami structures**. *Sci Rep* 2018, **8**:3378.

243. Hwang D-G, Trent K, Bartlett MD: **Kirigami-inspired structures for smart adhesion**. *ACS Appl Mater Interfaces* 2018, **10**:6747–6754.

244. Lamoureux A, Lee K, Shlian M, Forrest SR, Shtein M: **Dynamic kirigami structures for integrated solar tracking**. *Nat Commun* 2015, **6**:8092.

245. Song Z, Wang X, Lv C, An Y, Liang M, Ma T, He D, Zheng Y-J, Huang S-Q, Yu H, Jiang H: **Kirigami-based stretchable lithium-ion batteries**. *Sci Rep* 2015, **5**:10988.

246. Wang W, Li C, Rodrigue H, Yuan F, Han M-W, Cho M, Ahn S-H: **Kirigami/origami-based soft deployable reflector for optical beam steering**. *Adv Funct Mater* 2017, **27**:1604214.

247. Neville RM, Scarpa F, Pirrera A: **Shape morphing kirigami mechanical metamaterials**. *Sci Rep* 2016, **6**:31067.

248. * Kim J, Hanna JA, Byun M, Santangelo CD, Hayward RC: **Designing responsive buckled surfaces by halftone gel lithography**. *Science* 2012, **335**:1201–1205, https://doi.org/10.1126/science.1215309.
An excellent coupling of materials science and mechanics to direct the shape of microscopic structures.

249. Klein Y, Efrati E, Sharon E: **Shaping of elastic sheets by prescription of non-euclidean metrics**. *Science* 2007, **315**:1116–1120.

250. Holmes DP: *Active matter*. MIT Press; 2017:153–158.

251. Stein-Montalvo L, Costa P, Pezzulla M, Holmes DP: **Buckling of geometrically confined shells**. *Soft Matter* 2019, **15**:1215–1222.

252. Ge Q, Dunn CK, Qi HJ, Dunn ML: **Active origami by 4d printing**. *Smart Mater Struct* 2014, **23**. 094007.

253. Raviv D, Zhao W, McKnelly C, Papadopoulou A, Kadambi A, Shi B, Hirsch S, Dikovsky D, Zyracki M, Olguin C, *et al.*: **Active printed materials for complex self-evolving deformations**. *Sci Rep* 2014, **4**:7422.

254. Siéfert E, Reyssat E, Bico J, Roman B: **Bio-inspired pneumatic shape-morphing elastomers**. *Nat Mater* 2019, **18**:24.

255. Moulia B: **Leaves as shell structures: double curvature, auto-stresses, and minimal mechanical energy constraints on leaf rolling in grasses**. *J Plant Growth Regul* 2000, **19**: 19–30.

256. Dervaux J, Ciarletta P, Ben Amar M: **Morphogenesis of thin hyperelastic plates: a constitutive theory of biological growth in the Föppl von Kármán limit**. *J Mech Phys Solid* 2009, **57**: 458–471, https://doi.org/10.1016/j.jmps.2008.11.011.

257. Dervaux J, Couder Y, Guedeau-Boudeville M-A, Ben Amar M: **Shape transition in artificial tumors: from smooth buckles to singular creases**. *Phys Rev Lett* 2011, **107**:018103.

258. Armon S, Efrati E, Kupferman R, Sharon E: **Geometry and mechanics in the opening of chiral seed pods**. *Science (New York, N.Y.)* 2011, **333**:1726–1730, https://doi.org/10.1126/science.1203874.

259. Shorlin KA, de Bruyn JR, Graham M, Morris SW: **Development and geometry of isotropic and directional shrinkage crack patterns**. *Phys Rev* 2000, **61**:6950–6957.

260. Arnold W: **The cord moss and its allies**. *Bryologist* 1899, **2**: 52–55.

261. Setton LA, Tohyama H, Mow VC: **Swelling and curling behaviors of articular cartilage**. *J Biomech Eng Trans Asme* 1998, **120**:355–361.

262. King MJ, Vincent JFV, Harris W: **Curling and folding of leaves of monocotyledons - a strategy for structural stiffness**. *N Z J Bot* 1996, **34**:411–416.

263. Marder M: **The shape of the edge of a leaf**. *Found Phys* 2003, **33**:1743–1768, https://doi.org/10.1023/A:1026229605010.

264. Reyssat E, Mahadevan L: **Hygromorphs: from pine cones to biomimetic bilayers**. *J R Soc Interface* 2009, **6**:951–957.

265. Zhou Y, Lin G, Shih AJ, Hu SJ: **Assembly pressure and membrane swelling in PEM fuel cells**. *J Power Sources* 2009, **192**:544–551.

266. Holmes DP, Roché M, Sinha T, Stone H: **Bending and twisting of soft materials by non-homogenous swelling**. *Soft Matter* 2011, **7**:5188.

267. Dervaux J, Amar MB: **Mechanical instabilities of gels**. *Annual Rev Condens Matter Physics* 2012, **3**:311–332.

268. Pandey A, Holmes DP: **Swelling-induced deformations: a materials-defined transition from macroscale to microscale deformations**. *Soft Matter* 2013, **9**:5524.

269. Wu ZL, Moshe M, Greener J, Therien-Aubin H, Nie Z, Sharon E, Kumacheva E: **Three-dimensional shape transformations of hydrogel sheets induced by small-scale modulation of internal stresses**. *Nat Commun* 2013, **4**:1586–1587.

270. Pezzulla M, Shillig SA, Nardinocchi P, Holmes DP: **Morphing of geometric composites via residual swelling**. *Soft Matter* 2015, **11**:5812–5820.

271. Mora T, Boudaoud A: **Buckling of swelling gels**. *European Phys J E* 2006, **20**:119–124.

272. DuPont Jr SJ, Cates RS, Stroot PG, Toomey R: **Swelling-induced instabilities in microscale, surface-confined poly(N-isopropylacryamide) hydrogels**. *Soft Matter* 2010, **6**:3876.

273. Barros W, de Azevedo EN, Engelsberg M: **Surface pattern formation in a swelling gel**. *Soft Matter* 2012, **8**:8511.

274. ** Efrati E, Sharon E, Kupferman R: **Elastic theory of unconstrained non-Euclidean plates**. *J Mech Phys Solid* 2009, **57**: 762–775, https://doi.org/10.1016/j.jmps.2008.12.004.
Stimuli that leave a shell in a frustrated and residually stressed state cause strange and complex deformations. This model enables us to predict their shapes and stability.

275. Santangelo CD: **Buckling thin disks and ribbons with non-Euclidean metrics**. *Europhys Lett* 2009, **86**:34003.

276. Sharon E, Efrati E: **The mechanics of non-Euclidean plates**. *Soft Matter* 2010, **6**:5693, https://doi.org/10.1039/c0sm00479k.

277. Gemmer JA, Venkataramani SC: **Shape selection in non-Euclidean plates**. *Physica D* 2011, **240**:1536–1552.

278. Pezzulla M, Stoop N, Jiang X, Holmes DP: **Curvature-driven morphing of non-euclidean shells**. *Proc R Soc A* 2017, **473**: 20170087.

279. Dias MA, Hanna JA, Santangelo CD: **Programmed buckling by controlled lateral swelling in a thin elastic sheet**. *Phys Rev* 2011, **84**:1–7, https://doi.org/10.1103/PhysRevE.84.036603.

280. Douezan S, Wyart M, Brochard-Wyart F, Cuvelier D: **Curling instability induced by swelling**. *Soft Matter* 2011, **7**:1506.

281. Reyssat E, Mahadevan L: **How wet paper curls**. *EPL* 2011, **93**: 54001.

282. Kim J, Hanna JA, Hayward RC, Santangelo CD: **Thermally responsive rolling of thin gel strips with discrete variations in swelling**. *Soft Matter* 2012, **8**:2375.

283. Nah C, Lee GB, Lim CI, Ahn JH, Gent AN: **Swelling of rubber under nonuniform stresses and internal migration of swelling liquid when the stresses are removed**. *Macromolecules* 2011. 110218121457096.

284. Lucantonio A, Nardinocchi P: **Reduced models of swelling-induced bending of gel bars**. *Int J Solids Struct* 2012, **49**: 1399–1405.

285. ** Lucantonio A, Nardinocchi P, Teresi L: **Transient analysis of swelling-induced large deformations in polymer gels**. *J Mech Phys Solid* 2013, **61**:205–218.
Going beyond the linear poroelastic models of swelling, this stress diffusion approach is the best model I am aware of for describing the swelling of soft elastomers.

286. Tibbits S: **4d printing: multi-material shape change**. *Architect Des* 2014, **84**:116–121.

287. Khoo ZX, Teoh JEM, Liu Y, Chua CK, Yang S, An J, Leong KF, Yeong WY: **3d printing of smart materials: a review on recent progresses in 4d printing**. *Virtual Phys Prototyp* 2015, **10**: 103–122.

288. Bakarich SE, Gorkin III R, Panhuis MIH, Spinks GM: **4d printing with mechanically robust, thermally actuating hydrogels**. *Macromol Rapid Commun* 2015, **36**:1211–1217.

289. Gladman AS, Matsumoto EA, Nuzzo RG, Mahadevan L, Lewis JA: **Biomimetic 4d printing**. *Nat Mater* 2016, **15**:413.

290. Huang L, Jiang R, Wu J, Song J, Bai H, Li B, Zhao Q, Xie T: **Ultrafast digital printing toward 4d shape changing materials**. *Adv Mater* 2017, **29**:1605390.

291. Ding Z, Yuan C, Peng X, Wang T, Qi HJ, Dunn ML: **Direct 4d printing via active composite materials**. *Sci Adv* 2017, **3**. e1602890.

292. Poincloux S, Adda-Bedia M, Lechenault F: **Geometry and elasticity of a knitted fabric**. *Phys Rev X* 2018, **8**. 021075.

293. Dimitriyev M, Matsumoto E: **Geometry and mechanics of knitted fabric**. *Bull Am Phys Soc* 2018.

294. Baek C, Sageman-Furnas AO, Jawed MK, Reis PM: **Form finding in elastic gridshells**. *Proc Natl Acad Sci Unit States Am* 2018, **115**:75–80.

295. Mojdehi AR, Tavakol B, Royston W, Dillard DA, Holmes DP: **Buckling of elastic beams embedded in granular media**. *Extr Mech Lett* 2016, **9**:237–244.

296. Schunter Jr D, Brandenbourger M, Perriseau S, Holmes DP: **Elastogranular mechanics: buckling, jamming, and structure formation**. *Phys Rev Lett* 2018, **120**. 078002.

297. Algarra N, Karagiannopoulos PG, Lazarus A, Vandembroucq D, Kolb E: **Bending transition in the penetration of a flexible intruder in a two-dimensional dense granular medium**. *Phys Rev* 2018, **97**. 022901.

298. Kolb E, Hartmann C, Genet P: **Radial force development during root growth measured by photoelasticity**. *Plant Soil* 2012, **360**: 19–35.

299. Wendell D, Luginbuhl K, Guerrero J, Hosoi A: **Experimental investigation of plant root growth through granular substrates**. *Exp Mech* 2012, **52**:945–949.

300. Kolb E, Legué V, Bogeat-Triboulot M-B: **Physical root–soil interactions**. *Phys Biol* 2017, **14**. 065004.

301. Aejmelaeus-Lindström P, Willmann J, Tibbits S, Gramazio F, Kohler M: **Jammed architectural structures: towards large-scale reversible construction**. *Granul Matter* 2016, **18**:28.

302. Dierichs K, Menges A: **Towards an aggregate architecture: designed granular systems as programmable matter in architecture**. *Granul Matter* 2016, **18**:25.

303. Fauconneau M, Wittel FK, Herrmann HJ: **Continuous wire reinforcement for jammed granular architecture**. *Granul Matter* 2016, **18**:27.

304. Patrick JF, Hart KR, Krull BP, Diesendruck CE, Moore JS, White SR, Sottos NR: **Continuous self-healing life cycle in vascularized structural composites**. *Adv Mater* 2014, **26**: 4302–4308.

305. Diesendruck CE, Sottos NR, Moore JS, White SR: **Biomimetic self-healing**. *Angew Chem Int Ed* 2015, **54**:10428–10447.

306. Li W, Matthews CC, Yang K, Odarczenko MT, White SR, Sottos NR: **Autonomous indication of mechanical damage in polymeric coatings**. *Adv Mater* 2016, **28**:2189–2194.

307. Hauser AW, Evans AA, Na J-H, Hayward RC: **Photothermally reprogrammable buckling of nanocomposite gel sheets**. *Angew Chem Int Ed* 2015, **54**:5434–5437.

308. Hauser AW, Liu D, Bryson KC, Hayward RC, Broer DJ: **Reconfiguring nanocomposite liquid crystal polymer films with visible light**. *Macromolecules* 2016, **49**:1575–1581.

309. Jeon S-J, Hauser AW, Hayward RC: **Shape-morphing materials from stimuli-responsive hydrogel hybrids**. *Acc Chem Res* 2017, **50**:161–169.

310. Blonder G: **Non-linear temperature-dependent curvature of a phase change composite bimorph beam**. *Mater Res Express* 2017, **4**. 065704.

Supplementary Information: Elasticity and Stability of Shape Changing Structures

Douglas P. Holmes[a]

[a]*Department of Mechanical Engineering, Boston University, Boston, MA, 02215 USA*

1. A bit more on stretching & bending

Shell theories have a common structure: a stretching energy $\mathcal{U}_s$, which accounts for in–plane deformations, that is linear in the shell thickness, h, and a bending energy $\mathcal{U}_b$, which accounts for the curvature change of the deformed shell, and is dependent on h^3 [1, 2, 3, 4]. The dimensionless strain energy of the Koiter shell equations are written in covariant form as [5]

$$\mathcal{U}_s = \frac{Y}{2}\int\left[(1-\nu)\varepsilon^{\alpha\beta}\varepsilon_{\alpha\beta} + \nu(\varepsilon^{\alpha}_{\alpha})^2\right]\mathrm{d}\omega \sim Y\int\varepsilon^2\mathrm{d}\omega, \tag{1a}$$

$$\mathcal{U}_b = \frac{B}{2}\int\left[(1-\nu)\kappa^{\alpha\beta}\kappa_{\alpha\beta} + \nu(\kappa^{\alpha}_{\alpha})^2\right]\mathrm{d}\omega \sim B\int\kappa^2\mathrm{d}\omega, \tag{1b}$$

where $Y = Eh/(1-\nu^2)$ is the stretching rigidity, $B = Eh^3/[12(1-\nu^2)]$ is the bending rigidity, E is Young's elastic modulus, ν is Poisson's ratio, $\mathrm{d}\omega$ is the area element, and $\boldsymbol{\varepsilon}$ and $\boldsymbol{\kappa}$ are the tensors that describe the stretching and bending of the middle surface of the shell, respectively. The Greek indices $\alpha \in [1, 2]$, and raised indices refer to contravariant components of a tensor, while lowered indices refer to covariant components. The intricacies of this notation are not important upon a first introduction to this topic, but for the curious reader I would recommend the instructive text by Niordson [5]. I will elaborate on the covariance of the these tensors in the following section. The energies each contain the square of two invariants, since the shell is two–dimensional, for example with $\varepsilon^{\alpha}_{\alpha}$ being a measure of how the area changes and $\varepsilon^{\alpha\beta}\varepsilon_{\alpha\beta}$ being a measure of how the shell is distorted.

2. A brief note on covariance

Continuum mechanics is not often taught with a covariant framework, and so those not trained in physics, where this framework is at the heart of special and general relativity, the notation can be quite confounding. If space is flat, like a sheet of paper, then Cartesian coordinates are adequate to grasp much of the underlying principles. However, much is lost in this representation, and while the covariant framework of elasticity is terrifying for most, including myself, when they first encounter it, we can start making sense of the objects that this representation relies on without too much work. I am indebted to Einar Rødland on the Mathematics StackExchange for the analogies that follow [6].

Contravariance – Consider a map projection of the Earth, and so we are all on the same page, let's consider the Mercator projection. In this projection, land areas near the poles (such as Greenland and Antarctica) are severely stretched as compared to those around the equator. Let's assign a coordinate system x^{α} to identify the locations places on the surface of the Earth, where $\alpha, \beta \in 1, 2$ correspond to axes of longitude (along the horizontal) and latitude (along the vertical) with units of degrees. If we walk from East to West, the duration of our walk will be denoted by t, and we can determine our speed by $\dot{x}^{\alpha} = \mathrm{d}x^{\alpha}/\mathrm{d}t$. The vector $\dot{x}^{\alpha}$ is a *tangent* vector, which for convenience can be visualized as an arrow, with the length indicating the magnitude of our speed. These tangent vectors will be quite small while walking along the equator, and quite large while walking around the South Pole. Stretching parts on the map causes the tangent vectors to be stretched with it.

Covariance – Now, instead of concerning ourselves with our velocity as we walk, let's imagine we have measured the elevation at every point on Earth. By examining the gradient of elevation at points on Earth, we can draw contours that indicate regions where elevation is constant. Contours that are close together indicate a steep hill, while contours that are far apart indicate a flat plain. The gradient of elevation is a *covector*, and since it has units of elevation per distance, the contour lines will be far apart on the regions of map that are stretched (*e.g.* the South Pole). Stretching parts of the map causes the gradient, or covectors, to become less steep.

3. A bit more on elastic stability

Unfortunately, most student's first and only exposure to a problem of elastic stability is a rather deceptive one – the Euler buckling of a column. In studying the Euler buckling of a column, it is customary to make a one particularly significant assumption – that the column is *incompressible*. This assumption is advantageous because it is both reasonable, as most columns do not shorten significantly before buckling, and it simplifies the calculation. However, it is quite misleading, and I will let one of the forefathers of stability theory, W.T. Koiter explain why (emphasis mine):

> *"Here it appears that a negative second variation of the potential energy of the external loads is the cause of a loss of stability, but this state of affairs is due to our*

Email address: dpholmes@bu.edu (Douglas P. Holmes)
URL: www.bu.edu/moss (Douglas P. Holmes)

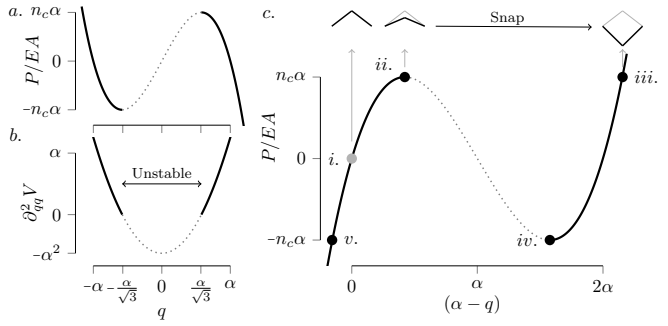

Figure 1: *a*. Normalized force P/EA plotted as a function of angle q showing extrema at $n_c\alpha$, where $n_c = -\frac{2\pi^3}{75\sqrt{3}}$. *b*. The second variation of the total potential energy is plotted as a function of angle q. The equilibrium configuration is unstable when $\partial^2_{qq} \leq 0$. *c*. Normalized force is plotted as a function of rotation, showing the loading path from *i*. the initial configuration to *ii*. the limit point at $n_c\alpha$, at which point stability is lost and the structure snaps to *iii*. Upon unloading from *iii*. to the limit point at *iv*. the structure snaps to *v*. Removal of the load restores the initial configuration *i*.

> *simplifying assumption of an incompressible rod, and we may not generalize this experience to other cases, as still happens only too frequently. In fact, in the case of elastic structures under dead loads the potential energy of the external loads does not enter at all into the stability condition.* **Loss of stability of elastic structures is always due to an internal exchange of energy.**" [7]

What that means physically is that it is the energy, and more specifically its second variation, in the *deformed* or *fundamental* state that needs to be evaluated for stability, and not the potential acting on the structure in its *original* or *reference* state. For a more fundamental and at times conceptual discussion of elastic stability, I recommend the two textbooks by Thompson and Hunt [8, 9].

4. The simplest snapping structure

The simplest structure that exhibits snapping is the bistable truss first analyzed by von Mises, in which two elastic bars of elastic modulus E, cross sectional area A, and an axial stiffness $EA/(L/\cos\alpha)$ are pinned together with an initial angle α, and pinned at supports separated by a distance $2L$. A force P applied to the apex of the truss will change the angle from α to q, and induce a compressive strain in the bars of $\varepsilon = \cos\alpha/\cos q - 1$, which causes a vertical displacement $w = L(\tan\alpha - \tan q)$. In this single degree of freedom example, the total potential energy is simply the strain energy in the spring minus the potential energy of the load,

$$V(q) = \frac{EAL}{\cos\alpha}\left(\frac{\cos\alpha}{\cos q} - 1\right)^2 - PL(\tan\alpha - \tan q). \tag{2}$$

Equilibrium is found by setting the first variation of the potential energy to zero,

$$\frac{\partial V}{\partial q} = \frac{L}{\cos^2 q}\left[2EA(\cos\alpha\tan q - \sin q) + P\right] = 0, \tag{3}$$

from which we can find the equilibrium path

$$\frac{P}{EA} = 2(\sin q - \cos\alpha\tan q), \tag{4}$$

which is plotted in figure 1a. Here we note an important distinction between snapping, which is a limit point instability, and buckling, which is a bifurcation – there is only one equilibrium path, meaning the truss will deflect under any infinitesimal load P. A system that exhibits a limit point instability has only one equilibrium path, and loss of stability will cause a discontinuous jump in a given parameter, *i.e.* a finite change in q in response to an infinitesimal change in P. Stability of this truss will be lost when the second variation of its potential energy, $\delta^2 V = \frac{1}{2!}\frac{\partial^2 V}{\partial q^2}\delta q^2$, ceases to be positive definite. We will evaluate the stability of the equilibrium state at a constant load by inserting the load from equation 4 into equation 3, and calculating the second variation of V as

$$\frac{\partial^2 V}{\partial q^2} = 2\frac{EAL}{\cos^4 q}\left(\cos\alpha - \cos^3 q\right), \tag{5}$$

which is plotted in which is plotted in figure 1b. It is clear from the graph that a region of this second variation is below zero, specifically when $-\alpha/\sqrt{3} \leq q \leq \alpha/\sqrt{3}$. This region of the equilibrium path given by equation 4 is unstable. Since in this example we have considered a load–controlled experiment, meaning the magnitude of the low is being increased, the truss has no choice but to jump (horizontally) from point *ii*. to point *iii*. on Fig. 1c., since this is the closest, stable part of the equilibrium curve at the same fixed value of P/EA.

In general, finding the critical point of a snap–through instability is a challenge, because when you linearize the equations you lose all information about the instability. This can be immediately seen with our simple example of the von Mises truss from equation 2 – a Taylor series expansion of q for any α leaves you with a linear equation, and thus the critical point is lost – its second variation will never be negative, so one would erroneously think the system is always stable. Numerically, there are multiple approaches for finding, following, and continuing through instability points [10], including utilizing arc–length methods or dynamic simulations.

5. The simplest buckling structure

To see the buckling and postbuckling behavior of a structure, it is useful to consider a nonlinear, finite–deflection theory – something that is straightforward to examine in a discrete, one degree of freedom system. Consider a rigid bar of length L that is held vertical by a rotational spring of stiffness k_r, and loaded at the free end of the bar by a a load P. If it is perfectly vertical, there is no initial inclination angle to the bar[1], *i.e.* $\alpha = 0$. We

[1] To consider the role of imperfections, or to analyze the stability of a whole array of structures and materials, I recommend pouring over the invaluable tome by Bažant and Cedolin [11], especially chapter 4.

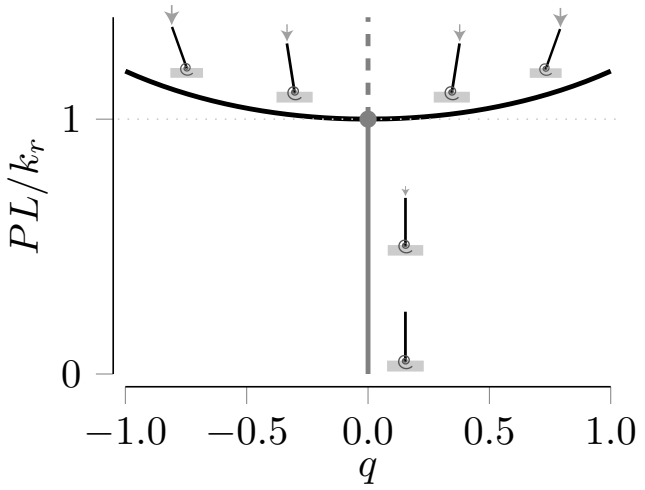

Figure 2: A plot of the two equilibrium curves of a buckling rigid bar, using the equilibrium paths given by equation 8. When $PL/k_r \leq 1$, the bar remains vertical, and it buckles either to the left ($q < 0$) or right ($q > 0$) when $PL/k_r > 1$. At the critical point, which is stable [8, 9], there is an exchange of stability between the gray equilibrium curve and the black curve as the structure buckles.

can again use q to measure the inclination angle of the bar after loading, so that the total potential energy may be written as

$$V(q) = \frac{1}{2}k_r q^2 - PL(1 - \cos q), \tag{6}$$

where the first term on the right hand side is the strain energy stored in the rotational spring, and the second term is the work of the load. Its first variation yields

$$\frac{\partial V}{\partial q} = k_r q - PL \sin q, \tag{7}$$

and since equilibrium requires the first variation to be stationary, *i.e.* $\partial V = 0$, we find the equilibrium relation between force and angle to be

$$P(q) = \frac{k_r}{L}\left(\frac{q}{\sin q}\right). \tag{8}$$

Upon inspection of equation 8, we see that there are two solutions that satisfy this equation: $q = 0$ or $q \neq 0$ (Fig. 2). The bar can stay perfectly vertical, *i.e.* $q = 0\ \forall\ P$, but that solution is not always stable. We can check the stability of our system by evaluating the second variation of V, and requiring it to be positive definite. The second variation is

$$\frac{\partial^2 V}{\partial q^2} = k_r - PL \cos q. \tag{9}$$

By setting this second variation equal to zero, we find the critical buckling force

$$P_c = \frac{k_r}{L \cos q}, \tag{10}$$

and by inserting equation 8 into equation 9 we see that this post-buckling path is stable for all q. For $P \leq P_c$, the bar will remain vertical and undeflected, and for $P > P_c$, the bar will buckle either to the left or the right, breaking symmetry, and this buckling direction will be dictated by imperfections in the bar or the eccentricity of the load.

6. Buckling of continuous structures

6.1. Elastica

The history behind the mathematical treatment of a thin elastic structure is rich, and a detailed discussion of it is well beyond the scope of this review. I would encourage all interested to read a history of it as detailed by Levien [12]. A nice recent article that revisited the mathematical intricacies of the problem was prepared by Singh *et al.* [13], along with a detailed derivation of the governing equations and various solutions in a recent book by Bigoni [14]. There are typically three flavors of equilibrium equations for the elastica, and their utility very much depends on either what community the research is embedded within, or how the particulars of a given problem lend themselves to a straightforward solution. In general, you will encounter the equations parameterized by the angle along the arc length of the elastic curve $\theta(s)$, the curvature along the arc length $\kappa(s)$, or through a force and moment balance. All three are equivalent and can be recovered with a little effort and some geometry – an exercise left up to the reader. For instance, a moment and force balance yields

$$\boldsymbol{m}'(s) + \hat{\boldsymbol{t}}(s) \times \boldsymbol{f}(s) = 0, \tag{11a}$$

$$\boldsymbol{f}'(s) + \hat{\boldsymbol{n}}(s) = 0, \tag{11b}$$

where $\boldsymbol{m}(s)$ and $\boldsymbol{f}(s)$ are the moments and forces acting on the curve, respectively, and $\hat{\boldsymbol{t}}(s)$ and $\hat{\boldsymbol{n}}(s)$ are the tangent and normal vectors along the curve, respectively. Here, we use an apostrophe to denote an ordinary derivative with respect to the arc length. Using the Frenet–Serret frame, the equations can be rewritten in terms of the curvature along the arc length as

$$2\kappa''(s) + \kappa^3 - \mu\kappa(s) + \sigma = 0, \tag{12}$$

where μ and σ are constants corresponding to how the elastica is loaded. Finally, this equation can in turn be shown to be equivalent to the equilibrium equation of a planar elastica as parameterized by the angle along the arc length as

$$\theta''(s) + \lambda_p^2 \sin\theta(s) = 0, \tag{13}$$

where s is the arc length that parameterizes the curve, θ is the angle that the tangent vector at a given point s makes with the horizon, and $\lambda_p^2 = P/B$ is the ratio of the applied load P to the bending rigidity B of the beam.

The buckling of an elastica, or an Euler column, is a problem encountered by most engineers during their studies. Its solution begins by linearizing equation 13, which is nonlinear because of the term $\sin\theta(s)$. Linearizing about the flat state allows us to consider small angles, such that $\sin\theta(s) \approx \theta(s)$, such that what started as a nonlinear eigenvalue problem now becomes a linear eigenvalue problem. For example, for an elastica that is simply

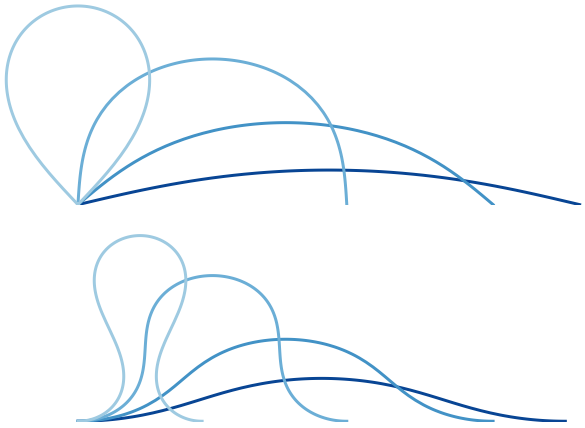

Figure 3: (Top) Shapes of a simply supported elastica subjected to various end shortenings. Graphs were generated in MATHEMATICA using equations 15a,b. (Bottom) Shapes of a clamped–clamped elastica subjected to various end shortenings. Graphs were generated in MATHEMATICA using equations 16a,b using the code block provided below these equations.

supported at its ends, the lowest eigenvalue is gives a critical buckling load of

$$P_c = \pi^2 \frac{B}{L^2}, \tag{14}$$

where L is the length of the elastica. For a clamped–clamped elastica, the buckling load is four times as large. Linearizing the equations comes at a cost, however – while we gain insight into the force at which buckling will occur, along with the mode shape of the buckled structure, we lose the ability to quantify the amplitude of the deflection.

The post–buckling shape of a simply supported elastica is determined by the parametric equations [14]

$$x(s) = \frac{2}{\Lambda(k)}(\mathcal{E}[\mathrm{am}[s\Lambda(k) + \mathcal{K}[k]|k]|k] - \mathcal{E}[am[\mathcal{K}[k], k], k]) - s, \tag{15a}$$

$$y(s) = -\frac{2}{\Lambda(k)} k\,\mathrm{cn}[s\Lambda(k) + \mathcal{K}[k]|k], \tag{15b}$$

where $k = \sin\frac{\alpha}{2}$, α is the angle of rotation at the inflection point at $s = L/2$, *i.e.* symmetry allows the analysis to focus on only half of the rod length, $\Lambda(k) = 2m\mathcal{K}[k]$ which for a mode one deformation $m = 1$, $\mathcal{K}[\cdot]$ is the complete elliptic integral of the first kind, $\mathcal{E}[\cdot|\cdot]$ is the incomplete elliptic integral of the second kind, $\mathrm{am}[\cdot|\cdot]$ is the amplitude for Jacobi elliptic functions, and $\mathrm{cn}[\cdot|\cdot]$ is the Jacobi cn elliptic function. Increasing α will increase the amplitude of the elastica while conserving the elastica's arc length. Similarly, the post–buckling shape of clamped–clamped elastica is then determined by the parametric equations [14]

$$x(s) = \frac{2}{\Lambda(k)}\mathcal{E}[\mathrm{am}[s\Lambda(k)|k]|k] - s, \tag{16a}$$

$$y(s) = \frac{2}{\Lambda(k)} k(1 - \mathrm{cn}[s\Lambda(k)|k]), \tag{16b}$$

where $k = \sin\frac{\alpha}{2}$, α is the angle of rotation at the inflection point at $s = L/4$, *i.e.* symmetry allows the analysis to focus on only quarter of the rod length, and $\Lambda(k) = 2(m+1)\mathcal{K}[k]$ which for a mode one deformation $m = 1$. Increasing α will increase the amplitude of the elastica while conserving the elastica's arc length. The following MATHEMATICA code is provided to enable the reader to visualize the deformed shape of the clamped–clamped elastica given by equations 16a

```
In[1]:= k[α_]:= Sin[α/2]

In[2]:= λc[k_, m_]:= 2 (m + 1) EllipticK[k]

In[3]:= xc[s_, α_, m_]:= (-s +
          2/λc[k[α],
            m] (EllipticE[JacobiAmplitude[
            s λc[k[α], m], k[α]], k[α]]))

In[4]:= yc[s_, α_, m_]:= (2 k[α]/λc[k[α],
            m] (1 - JacobiCN[s λc[k[α], m],
            k[α]]))

In[5]:= ParametricPlot[
        {xc[s, 1.5, 1], yc[s, 1.5, 1]},
         {s, 0, 1}]
```

where for the parametric plot, values of $\alpha = 1.5$ and mode number of $m = 1$ were chosen arbitrarily. Example elastica curves are plotted in Fig. 3.

In both the simply supported and clamped–clamped case, the end shortening $u(\alpha)/L$ is given by

$$\frac{u(\alpha)}{L} = 2\left(1 - \frac{\mathcal{E}(k)}{\mathcal{K}(k)}\right). \tag{17}$$

6.2. *Plates & Shells*

We began this review with Koiter's thin shell equations, *i.e.* equations 1a and 1b. There are various simplifications that can be made to these equations to make them more mathematically tractable [5], and we will begin with a commonly used set of equations to describe the mechanics of thin plates: the Föppl-von Kármán (FvK) plate equations. The FvK equations are rooted in an approximation for the plate's in–plane strain $\varepsilon_{\alpha\beta}$ where the non–linear terms describing the plate's out–of–plane deflection w are retained, while the non–linear terms corresponding to the plate's in–plane displacements u_α are discarded, such that $\varepsilon_{\alpha\beta} \approx 1/2(u_{\alpha,\beta} + u_{\beta,\alpha} + w_{,\alpha}w_{,\beta})$, where the comma represents differentiation, *i.e.* $f_{,\alpha} \equiv \partial f/\partial x_\alpha$. Using the FvK approximation for strain, a plate's equilibrium equations can be arrived at from a variational approach that minimizes the plate's free energy [15].

$$B\nabla^4 w - h\sigma_{\alpha\beta}w_{,\alpha\beta} = 0, \tag{18a}$$

$$\sigma_{\alpha\beta,\beta} = 0, \tag{18b}$$

where $B = Eh^3/12(1-\nu^2)$ is the bending stiffness. Alternatively, by introduction of the Airy potential, $\sigma_{\alpha\beta} = \epsilon_{\alpha\gamma}\epsilon_{\beta\mu}\phi_{,\lambda\mu}$, where $\epsilon_{\alpha\beta}$ is the two–dimensional Levi–Civita symbol, and the "die" operator, which represents a symmetric contraction of two

components,*i.e.* $\diamondsuit^4[f,g] \equiv f_{,\alpha\alpha}g_{,\beta\beta} - 2f_{,\alpha\beta}g_{,\alpha\beta} + f_{,\beta\beta}g_{,\alpha\alpha}$ [16], the equilibrium equations can be written as

$$B\nabla^4 w - \diamondsuit^4[\phi, w] = 0, \tag{19a}$$

$$\frac{1}{Y}\nabla^4\phi + \frac{1}{2}\diamondsuit^4[w,w] = 0, \tag{19b}$$

where $Y = Eh$ is the stretching stiffness. These equations are non–linear, with the term $\diamondsuit^4[\phi, w]$ coupling the plate's curvature with in–plane stress, and the term $\diamondsuit^4[w,w]/2$ representing the Gauss curvature K. The explicit appearance of the Gauss curvature illustrates the intimate connection between a plate's elasticity and its geometry [17], and this interplay will consistently appear in the various examples that follow.

A plate is a thin structure that is flat in its stress–free configuration, while a shell has a non–zero initial curvature. An instructive approach to the complexities that arise with shell mechanics is to regard the shell as consisting of two distinct surfaces: one which sustains *stretching* stress resultants and the other which sustains the *bending* stress resultants. Calladine [18] covers this *two–surface* approach to the equilibrium equations for shells in a comprehensive manner, and we will only highlight the key components here. In this two–surface approach, the stretching surface is equivalent to the membrane hypothesis of shells, and the bending surface is very similar to the FvK analysis detailed above. The general interaction between these two imaginary surfaces, *i.e.* the way an externally applied force is distributed between them, leads directly to the Donnell–Mushtari–Vlasov (DMV) equations [19].

$$B\nabla^4 w + \nabla_k^2\phi - \diamondsuit^4[\phi, w] = 0, \tag{20a}$$

$$\frac{1}{Y}\nabla^4\phi - \nabla_k^2 w + \frac{1}{2}\diamondsuit^4[w,w] = 0. \tag{20b}$$

These equilibrium equations contain the Vlasov operator $\nabla_k^2(f) \equiv R_\beta^{-1} f_{,\alpha\alpha} + R_\alpha^{-1} f_{,\beta\beta}$, which incorporates the shell's principal curvatures. It should be immediately apparent that in the absence of any initial curvature, equations 20a and 20b revert directly to the FvK equations given by equations 19a and 19b. Since these equations are an extension of the FvK plate equations, they retain the same variational structure, and are applicable under similar assumptions of small strains and moderate rotations [17].

Few exact solutions to the Föppl-von Kármán equations are known to exist, but geometrical simplifications make the FvK equations useful for describing the Euler buckling of a plate in response to an in–plane stress. A uniaxially compressed plate that buckles out–of–plane will have cylindrical symmetry, which greatly simplifies the geometry, since a cylindrical shape is developable to a plane, such that in equation 19b $K = \diamondsuit^4[w,w]/2 = 0$. Since there is only stress in one direction, say the x–direction, equation 19b reduces to $\phi_{,xxxx} = 0$. Considering a plate with clamped boundary conditions, this equation for ϕ can be integrated, allowing equation 19a to reduce to an ordinary differential equation, which can be solved in terms of the plate's deflection [17],

$$w(x,y) = \pm\frac{h}{\sqrt{3}}\left(\frac{\sigma}{\sigma_{Eu}} - 1\right)^{1/2}\left(1 + \cos\frac{\pi x}{L}\right), \tag{21}$$

where L is the length of the plate, σ is the uniaxial stress, and the Euler buckling stress is

$$\sigma_{Eu} = \frac{\pi^2 E}{3(1-\nu^2)}\left(\frac{h}{L}\right)^2. \tag{22}$$

As noted in the subsection on *Warping Wafers*, buckling of thin plates can also occur from a mismatch of strains through the thickness, in particular with heated or differentially swollen plates. Some additional, relevant references to this topic include [20, 21, 22, 23, 24, 25].

6.3. Wrinkling

When a thin plate is bound to a compliant substrate and compressed, higher buckling modes emerge, and the pattern formation of these ordered buckled structures, or wrinkles, have garnered significant recent interest. The wavelength of wrinkles is selected by a balance of plate's bending energy and the energy required to deform the underlying elastic substrate. The bending resistance of the sheet penalizes short wavelengths, while deformation of the elastic foundation that is supporting the sheet penalizes long wavelengths. An intermediate wavelength emerges when we consider that the reaction of the underlying layer K is proportional to the deflection of the plate w. In the simplest case, for 1D wrinkles extending in the x–direction, equation 18a becomes

$$Bw_{,xxxx} - h\sigma_{xx}w_{,xx} + Kw = 0, \tag{23}$$

when a Winkler foundation is included [26]. By linearizing this equation, and discarding any stretching of the mid–plane due to curvature, *i.e.* the second term is zero, a characteristic length scale emerges based on a balance of the two rigidities. The scaling we found in equation 11 can be recovered here from dimensional analysis. In the limit of wrinkles on a very deep substrate, *i.e.* $h \ll \lambda \ll H_s$, the stiffness of the elastic foundation scales as $K \sim E_s/\lambda$ [27], and the wrinkle wavelength therefore scales as

$$\lambda \sim h\left(\frac{E}{E_s}\right)^{1/3}. \tag{24}$$

We can explicitly determine the critical stress required for wrinkles to form and the resulting wavelength by linearizing equations 18a and 18b about the flat, unbuckled state, *i.e.* $u_\alpha = w = 0$, and performing linear stability analysis [28, 29, 30, 31, 32, 33, 34]. Linearizing these equations requires the strain tensor to simplify to $\varepsilon_{\alpha\beta} \approx 1/2(u_{\alpha,\beta} + u_{\beta,\alpha})$. The plate will be considered infinite in the x_α directions, and exposed to equibiaxial stress, such that the linearized equations are $B\nabla^4 w - h\sigma_0\nabla^2 w = -p$ and $\nabla^4\phi = 0$. The stress component exerted by the substrate onto the plate is introduced as p. These ordinary differential equations allow periodic solutions in the form $w(x,y) = \hat{w}\cos(k_1 x)$, which result in a cylindrical pattern described by a critical threshold σ_c and wavelength λ

given by [35, 29, 30, 32]

$$\sigma_c = E^* \left(\frac{3E_s^*}{2E^*} \right)^{2/3}, \tag{25a}$$

$$\lambda = \pi h \left(\frac{2E^*}{3E_s^*} \right)^{1/3}. \tag{25b}$$

The starred quantities E^* and E_s^* represent the effective, or reduced, modulus of the plate and substrate, respectively. The reduced modulus of the plate is $E^* = E[1 - \nu^2]^{-1}$, while the reduced modulus of the substrate includes the tangential traction forces exerted by the substrate onto the plate, such that $E_s^* = E_s(1 - \nu_s)[(1 + \nu_s)(3 - 4\nu_s)]^{-1}$ [31, 32, 33].

Wrinkles that form under compression are familiar to most everyone – they appear by simply compressing our skin. It is less intuitive to observe wrinkles that form as a free elastic sheet is pulled in tension [36, 37, 27, 38]. This problem is no longer confined to 1D as there is a tension T in the y–direction, and localized regions of compressive in the x–direction near the clamped boundaries. The equilibrium equation that emerges from minimizing the free energy for this configuration is $Bw_{,xxxx} - h\sigma_{xx}w_{,xx} - Tw_{,yy} = 0$ [27]. Cerda *et al.* [27] identified an analogy between the energy in an elastic foundation supporting a thin sheet, $U_f \sim \int_A Kw^2 \, \mathrm{d}A$,and the sheet's stretching energy, $U_m \sim \int_A T\,(w_{,x})^2 \, \mathrm{d}A$. Since these energies are of similar form, and with the in–plane strain scaling as $w_{,x} \sim w/L$, comparing the two leads to the emergence of *effective* stiffness of the elastic foundation, $K \sim T/L^2$. This connection is convenient as it allows equation 23, and the scaling in equation 24, to hold for a variety of wrinkling problems, with each problem varying only in the actual form of the effective stiffness of the elastic foundation, K.

6.4. Folding

As the amount of overstress, or confinement, of the compressed plate increases, the bending energy along the plate goes from being broadly distributed among wrinkles to being localized within sharper features [39, 40, 41, 42, 43, 44, 45, 46, 47, 48, 49, 50, 51, 52, 53, 54]. When the compressive strain exceeds a critical value of $\varepsilon \simeq 0.2$, a pitchfork bifurcation of the wrinkle morphology emerges as one wrinkle grows in amplitude while neighboring wrinkles decrease [40, 41, 42]. This focusing of bending energy leads to a break in the up–down symmetry of the wrinkled plate, and is analogous to period–doubling bifurcations in dynamical systems [42]. The symmetry breaking occurs from the nonlinear contribution of the compliant foundation that supports the stiff plate as the out–of–plane deflection and in–plane compression of the plate are no longer equivalent [42, 50]. Further compression of the plate beyond a strain of $\varepsilon \simeq 0.26$ leads to a period-quadrupling bifurcation [42], in which sharp folds appear, localizing the much of the stress within highly curved ridges [55, 40, 41, 42, 56, 50]. This folding is a means for focusing the elastic energy within the plate. Qualitatively, a fold occurs when the radius of curvature of the deformed feature is on the same order as the thickness of the film.

When folds occur over a large scale, for instance with the crumpling of a piece of paper, these stress-focused ridges can significantly alter the mechanical properties of the structure. A crumpled piece of paper is characterized by sharp ridges that terminate at point–like singularities. These singularities are conical dislocations, and they emerge as the sheet tries to resist stretching, thereby localizing the stretched region into the tip of the cone. Referred to as *developable cones*, or *d–cones*, due to their isometry to a flat plate, the shape is a particular solution to the FvK equations in the limit of large deflections [57, 58, 59, 60, 61]. A d–cone is a building block to a crumpled sheet, and two of these singularities are connected by a stretching ridge, which contains much of the deformation energy within a strongly buckled sheet [62, 63, 64]. The width of these stretching ridges can be arrived at either by scaling considerations of the sheets elastic energy [63] or by a boundary layer analysis of the FvK equations [65]. Upon formation of a ridge, the bending and stretching energies are of the same order, and for a sharp fold on a plate with a given thickness, these energies will scale linearly with the crease length χ, *i.e.* $U_m \sim U_b \propto \chi$. In reality, the curvature of the fold is softened by a small amount of stretching along the ridge, and as the length of the fold increases these energies grow at a slower rate, $U_m \sim U_b \propto \chi^{1/3}$ [62, 63, 65, 64]. Recent work has focused on the dynamic deformations of d–cones and ridges [66, 67], the interactions of disclinations and e-cones in extensible sheets [68], the existence and annihilation of multiple singularities in a constrained elastic plate to minimize stretching [69, 70], the mechanics of curved–folds [71], the nature of dipoles in thin sheets [72], and the appearance of a state variable for characterizing crumpled sheets [73].

[1] W. Koiter, A consistent first approximation in the general theory of thin elastic shells, Theory of thin elastic shells (1960) 12–33.

[2] W. T. Koiter, On the nonlinear theory of thin elastic shells. i, ii, & iii, Proceedings of the Koninklijke Nederlandse Akademie van Wetenschappen, Series B 69 (1) (1966) 1–54.

[3] W. Koiter, General equations of elastic stability for thin shells, in: Proceedings, Symposium on the Theory of Shells to Honor Lloyd Hamilton Donnett, 1967, pp. 1S7–230.

[4] W. T. Koiter, J. G. Simmonds, Foundations of shell theory, Springer Berlin Heidelberg, Berlin, Heidelberg, 1973, pp. 150–176.

[5] F. I. Niordson, Shell theory, Elsevier, 1985.

[6] E. Rødland, *understanding* covariance vs. contravariance.
URL `https://math.stackexchange.com/a/192308`

[7] B. Budiansky, Buckling of Structures: Symposium Cambridge/USA, June 17–21, 1974, Springer Science & Business Media, 2013.

[8] J. M. T. Thompson, G. W. Hunt, A general theory of elastic stability, London: J. Wiley, 1973.

[9] J. M. T. Thompson, G. W. Hunt, Elastic instability phenomena, Vol. 2, Wiley Chichester, 1984.

[10] E. Riks, An incremental approach to the solution of snapping and buckling problems, International Journal of Solids and Structures 15 (7) (1979) 529–551.

[11] Z. P. Bažant, L. Cedolin, Stability of structures: elastic, inelastic, fracture and damage theories, World Scientific, 2010.

[12] R. Levien, The elastica: a mathematical history, University of California, Berkeley, Technical Report No. UCB/EECS-2008-103.

[13] H. Singh, J. Hanna, On the planar elastica, stress, and material stress, arXiv preprint arXiv:1706.03047.

[14] D. Bigoni, Extremely Deformable Structures, Vol. 562, Springer, 2015.

[15] L. D. Landau, E. M. Lifshitz, Course of Theoretical Physics Vol 7: Theory and Elasticity, Pergamon Press, 1959.

[16] E. H. Mansfield, The bending and stretching of plates, Cambridge Uni-

versity Press, 1989.
[17] B. Audoly, Y. Pomeau, Elasticity and geometry, Oxford Univ. Press, 2010.
[18] C. R. Calladine, Theory of shell structures, Cambridge University Press, 1989.
[19] S. W., Vibrations of Shells and Plates, Marcel Dekker, 2004.
[20] E. H. Mansfield, Bending, buckling and curling of a heated thin plate, Proc. R. Soc. Lond. A 268 (1334) (1962) 316–327.
[21] E. H. Mansfield, Bending, buckling and curling of a heated elliptical plate, Proc. R. Soc. Lond. A 288 (1414) (1965) 396–417.
[22] C. B. Masters, N. Salamon, Geometrically nonlinear stress-deflection relations for thin film/substrate systems, International journal of engineering science 31 (6) (1993) 915–925.
[23] N. Salamon, C. B. Masters, Bifurcation in isotropic thinfilm/substrate plates, International journal of solids and structures 32 (3-4) (1995) 473–481.
[24] L. Freund, Substrate curvature due to thin film mismatch strain in the nonlinear deformation range, Journal of the Mechanics and Physics of Solids 48 (6-7) (2000) 1159–1174.
[25] K. Seffen, R. McMahon, Heating of a uniform wafer disk, International Journal of Mechanical Sciences 49 (2) (2007) 230–238.
[26] D. A. Dillard, B. Mukherjee, P. Karnal, R. C. Batra, J. Frechette, A review of winkler's foundation and its profound influence on adhesion and soft matter applications, Soft matter 14 (19) (2018) 3669–3683.
[27] E. Cerda, L. Mahadevan, Geometry and physics of wrinkling, Physical review letters 90 (7) (2003) 074302.
[28] H. G. Allen, Analysis and design of structural sandwich panels, Pergemon, New York, 1969.
[29] X. Chen, J. W. Hutchinson, A family of herringbone patterns in thin films, Scripta Materialia 50 (6) (2004) 797–801.
[30] X. Chen, J. W. Hutchinson, Herringbone Buckling Patterns of Compressed Thin Films on Compliant Substrates, Journal of Applied Mechanics 71 (5) (2004) 597–603.
[31] B. Audoly, A. Boudaoud, Buckling of a stiff film bound to a compliant substrate part i:, Journal of the Mechanics and Physics of Solids 56 (7) (2008) 2401–2421. doi:10.1016/j.jmps.2008.03.003.
[32] B. Audoly, A. Boudaoud, Buckling of a stiff film bound to a compliant substrate part ii:, Journal of the Mechanics and Physics of Solids 56 (7) (2008) 2422–2443. doi:10.1016/j.jmps.2008.03.002.
[33] B. Audoly, A. Boudaoud, Buckling of a stiff film bound to a compliant substrate part iii:, Journal of the Mechanics and Physics of Solids 56 (7) (2008) 2444–2458. doi:10.1016/j.jmps.2008.03.001.
[34] S. Cai, D. Breid, A. J. Crosby, Z. Suo, J. W. Hutchinson, Periodic patterns and energy states of buckled films on compliant substrates, Journal of the Mechanics and Physics of Solids 59 (5) (2011) 1094–1114.
[35] J. Groenewold, Wrinkling of plates coupled with soft elastic media, Physica A 298 (2001) 32–45.
[36] N. Friedl, F. G. Rammerstorfer, F. D. Fischer, Buckling of stretched strips, Computers Structures 78 (2000) 185–190.
[37] E. Cerda, K. Ravi-Chandar, L. Mahadevan, Thin films: Wrinkling of an elastic sheet under tension, Nature 419 (6907) (2002) 579.
[38] V. Nayyar, K. Ravi-Chandar, R. Huang, Stretch-induced stress patterns and wrinkles in hyperelastic thin sheets, International Journal of Solids and Structures 48 (25-26) (2011) 3471–3483.
[39] J. Huang, M. Juszkiewicz, W. H. De Jeu, E. Cerda, T. Emrick, N. Menon, T. P. Russell, Capillary wrinkling of floating thin polymer films, Science 317 (5838) (2007) 650–653.
[40] L. Pocivavsek, R. Dellsy, A. Kern, S. Johnson, B. Lin, K. Y. C. Lee, E. Cerda, Stress and Fold Localization in Thin Elastic Membranes, Science 320 (5878) (2008) 912–916.
[41] D. P. Holmes, A. J. Crosby, Draping Films: A Wrinkle to Fold Transition, Physical Review Letters 105 (3) (2010) 038303.
[42] F. Brau, H. Vandeparre, A. Sabbah, C. Poulard, A. Boudaoud, P. Damman, Multiple-length-scale elastic instability mimicsparametric resonance of nonlinear oscillators, Nature Physics 7 (1) (2010) 56–60.
[43] J. Huang, B. Davidovitch, C. D. Santangelo, T. P. Russell, N. Menon, Smooth Cascade of Wrinkles at the Edge of a Floating Elastic Film, Physical Review Letters 105 (3) (2010) 038302.
[44] D. Vella, M. Adda-Bedia, E. Cerda, Capillary wrinkling of elastic membranes, Soft Matter 6 (22) (2010) 5778.
[45] B. Davidovitch, R. D. Schroll, D. Vella, M. Adda-Bedia, E. A. Cerda, Prototypical model for tensional wrinkling in thin sheets., Proceedings of the National Academy of Sciences of the United States of America 108 (45) (2011) 18227–32. doi:10.1073/pnas.1108553108.
[46] B. Davidovitch, R. D. Schroll, E. Cerda, Nonperturbative model for wrinkling in highly bendable sheets, Physical Review E 85 (6) (2012) 066115. doi:10.1103/PhysRevE.85.066115.
[47] H. King, R. D. Schroll, B. Davidovitch, N. Menon, Elastic sheet on a liquid drop reveals wrinkling and crumpling as distinct symmetry-breaking instabilities, Proceedings of the National Academy of Sciences 109 (25) (2012) 9716–9720.
[48] Y. Ebata, A. B. Croll, A. J. Crosby, Wrinkling and strain localizations in polymer thin films, Soft Matter 8 (35) (2012) 9086.
[49] R. D. Schroll, M. Adda-Bedia, E. Cerda, J. Huang, N. Menon, T. P. Russell, K. B. Toga, D. Vella, B. Davidovitch, Capillary Deformations of Bendable Films, Physical Review Letters 111 (1) (2013) 014301.
[50] H. Diamant, T. a. Witten, Shape and symmetry of a fluid-supported elastic sheet, Physical Review E 88 (1) (2013) 012401.
[51] D. Vella, J. Huang, N. Menon, T. P. Russell, B. Davidovitch, Indentation of ultrathin elastic films and the emergence of asymptotic isometry, Physical review letters 114 (1) (2015) 014301.
[52] J. D. Paulsen, E. Hohlfeld, H. King, J. Huang, Z. Qiu, T. P. Russell, N. Menon, D. Vella, B. Davidovitch, Curvature-induced stiffness and the spatial variation of wavelength in wrinkled sheets, Proceedings of the National Academy of Sciences 113 (5) (2016) 1144–1149.
[53] F. Box, D. Vella, R. W. Style, J. A. Neufeld, Indentation of a floating elastic sheet: geometry versus applied tension, Proc. R. Soc. A 473 (2206) (2017) 20170335.
[54] D. Vella, B. Davidovitch, Regimes of wrinkling in an indented floating elastic sheet, arXiv preprint arXiv:1804.03341.
[55] T. Witten, Stress focusing in elastic sheets, Reviews of Modern Physics 79 (2) (2007) 643–675. doi:10.1103/RevModPhys.79.643.
[56] A. D. Cambou, N. Menon, Three-dimensional structure of a sheet crumpled into a ball, Proceedings of the National Academy of Sciences 108 (36) (2011) 14741–14745. doi:10.1073/pnas.1019192108.
URL http://www.pnas.org/cgi/doi/10.1073/pnas.1019192108
[57] M. Ben Amar, Y. Pomeau, Crumpled paper, in: Proceedings of the Royal Society of London-A- . . . , 1997, pp. 729–755.
[58] E. Cerda, L. Mahadevan, Conical surfaces and crescent singularities in crumpled sheets, Physical Review Letters 80 (11) (1998) 2358.
[59] S. Chaïeb, F. Melo, J.-C. Géminard, Experimental study of developable cones, Physical review letters 80 (11) (1998) 2354.
[60] E. Cerda, S. Chaieb, F. Melo, L. Mahadevan, Conical dislocations in crumpling, Nature 401 (6748) (1999) 46–49.
[61] S. Chaieb, From creases to conical deflections in a buckled thin sheet: stress focusing vs singularities in strong deformations of a thin elastic sheet, Journal of the Mechanics and Physics of Solids 48 (2000) 565–579.
[62] T. A. Witten, H. Li, Asymptotic Shape of a Fullerene Ball, Europhysics Letters (EPL) 23 (1) (1993) 51–55.
[63] A. Lobkovsky, S. Gentges, H. Li, D. Morse, T. A. Witten, Scaling Properties of Stretching Ridges in a Crumpled Elastic Sheet, Science 270 (5241) (1995) 1482–1485.
[64] A. E. Lobkovsky, T. A. Witten, Properties of ridges in elastic membranes, Physical Review E 55 (2) (1997) 1577–1589.
[65] A. Lobkovsky, Boundary layer analysis of the ridge singularity in a thin plate, Physical Review E 53 (4) (1996) 3750–3759.
[66] E. Hamm, B. Roman, F. Melo, Dynamics of developable cones under shear, Physical Review E 70 (2) (2004) 026607.
[67] A. Boudaoud, E. Hamm, F. Melo, Developable Modes in Vibrated Thin Plates, Physical Review Letters 99 (25).
[68] J. Chopin, A. Kudrolli, Disclinations, e-cones, and their interactions in extensible sheets, Soft matter 12 (19) (2016) 4457–4462.
[69] A. Boudaoud, P. Patricio, Y. Couder, M. Ben Amar, Dynamics of singularities in a constrained elastic plate, Nature 407 (6805) (2000) 718–720.
[70] L. Walsh, R. Meza, E. Hamm, Weakening of a thin shell structure by annihilating singularities, Journal of Physics D: Applied Physics 44 (23) (2011) 232002.
[71] M. A. Dias, C. D. Santangelo, The shape and mechanics of curved-fold origami structures, Europhysics Letters (EPL) 100 (5) (2012) 54005.
[72] J. Guven, J. Hanna, O. Kahraman, M. M. Müller, Dipoles in thin sheets, The European Physical Journal E 36 (9) (2013) 106.

[73] O. Gottesman, J. Andrejevic, C. H. Rycroft, S. M. Rubinstein, A state variable for crumpled thin sheets, Communications Physics 1 (1) (2018) 70.